A High-Accuracy Symplectic Scheme for a nonlinear transport problem

Farjana Siddiqua[1*] and Catalin Trenchea[2]

[1,2*]Mathematics, University of Pittsburgh, 301 Thackeray Hall, Pittsburgh, 15260, Pennsylvania, USA.

*Corresponding author(s). E-mail(s): fas41@pitt.edu;
Contributing authors: trenchea@pitt.edu;

Abstract

We analyze an advection-diffusion-reaction problem with non-homogeneous boundary conditions that models the chromatography process. We prove stability and error estimates for both constant and affine adsorption, using the symplectic one-step implicit midpoint method for time discretization and finite elements for spatial discretization. In addition, we perform the stability analysis for the nonlinear, explicit adsorption in the continuous and semi-discrete cases. For the nonlinear, explicit adsorption, we also complete the error analysis for the semi-discrete case and prove the existence of a solution for the fully discrete case. The numerical tests validate our theoretical results.

Keywords: Advection, Diffusion, Reaction, Chromatography, Adsorption

1 Introduction

The global market for biopharmaceuticals is expanding fast, and 50% of top 100 drugs will most likely be derived from biotechnology [1, 2]. The high demand for biopharmaceuticals is due to their effectiveness in treating various illnesses such as diabetes, anemia, cancer, etc. [3]. For example, monoclonal antibodies [4] are very useful medications in treating COVID-19 [5–7]. Other key factors driving the growth of the market are the rising investments in research and development of novel treatments, favorable government regulations, and the increasing adoption of biopharmaceuticals by the global population [1]. To maximize the production capacity while minimizing costs, manufacturers are constantly developing new methods. Integrating new technologies into existing facilities is more economically viable than the alternative of constructing new biomanufacturing facilities, due to financial risks. Upstream and downstream processes are typically part of a biomanufacturing facility. In the upstream process, cells cultured by genetically engineered methods release the desired product into a solution, and in the downstream process, the product is purified from the solution [8]. The capacity of production is often limited by downstream purification, usually including chromatography. In the protein chromatography process, when the solution is pushed through the column, the materials in columns separate the proteins [9]. The ideal media for the chromatography columns are resin beds, monoliths, and membranes [10]. Membrane chromatography [11–13] addresses the low efficiency of resin chromatography and uses a porous, absorptive membrane as the packing medium instead of the small resin beads. The protein binding capacity is crucial in membrane chromatography as it determines the volume of membrane required for purification. Most adsorption mechanisms, such as ion-exchange membranes, lose the protein binding capacity at relatively low conductivity and often require additional processing stages, causing lower yield and higher production costs. Recent advances in downstream bioprocessing have underscored the need for quantitative modeling frameworks that can predict solute transport and adsorption behavior within chromatographic membranes and resins. Nonlinear adsorption isotherms, such as Langmuir and steric mass-action (SMA) models, capture the competitive and capacity-limited binding [14–16]. The governing advection–diffusion–reaction equations considered in this paper are consistent with those derived for membrane chromatography columns, where mass transport resistance and nonlinear binding kinetics jointly determine the dynamic binding capacity and breakthrough performance [17, 18]. Mathematical analyses of these systems are essential for optimizing column design and predicting the performance of emerging multimodal membranes used for antibody and protein purification [19, 20]. The recent research in [12] focuses on multimodal membrane-based chromatography. The development of a modeling framework capable of characterizing the chromatography process under continuous flow circumstances is critical. In this paper, we model this process for creating a simulation tool for transport in a porous medium by adopting the reactive transport (advection-diffusion-reaction) problem in [9]. Our analysis can be relevant to general nonlinear transport problems, related to variable saturation flow models, e.g. Richards's equation, black oil and multiphase models in poroelastic media [21–29].

Let Ω be a bounded domain in $\mathbf{R}^{\mathbf{d}}$, where $d = 1,\ 2$, or 3, see Figure 1, with piecewise smooth boundary Γ. We partition the boundary into three non-overlapping parts $\Gamma = \Gamma_{\text{in}} \cup \Gamma_{\text{n}} \cup \Gamma_{\text{out}}$, where the inflow boundary is $\Gamma_{\text{in}} = \{x \in \Gamma : \overrightarrow{n} \cdot \mathbf{u}(x) < 0\}$, the outflow boundary is $\Gamma_{\text{out}} = \{x \in \Gamma : \overrightarrow{n} \cdot \mathbf{u}(x) > 0\}$, and the boundaries comprising no-flow hydraulic zone(s) are $\Gamma_{\text{n}} = \Gamma \backslash (\Gamma_{\text{in}} \cup \Gamma_{\text{out}})$. Let $\mathbf{u}$ denote the fluid velocity through the membrane, and $\overrightarrow{n}$ denote the unit outward normal to Ω. We assume that $\mathbf{u}$ is given, computed by the Darcy law [30], and satisfying the incompressibility condition $\boldsymbol{\nabla} \cdot \mathbf{u} = 0$, and $\mathbf{u} \cdot \overrightarrow{n}(x,t) = 0,\ \ x \in \Gamma_{\text{n}},\ t > 0$. Let ω be the total porosity of the membrane $(0 \leq \omega \leq 1)$, ρ_s be the density of the membrane, D be the diffusion tensor that represents the diffusivity of fluid through the membrane, C and $q(C)$ be the concentration in the liquid and absorbed phases respectively. For a forcing function

$f \in L^2(0,T;L^2(\Omega))$, given velocity $\mathbf{u}$ and initial concentration $C_0 \in L^2(\Omega)$, we consider the following initial boundary value problem of finding the concentration $C(x,t)$:

$$\begin{cases} \omega\partial_t C + (1-\omega)\rho_s\partial_t q(C) + \boldsymbol{\nabla}\cdot(\mathbf{u}C) - \boldsymbol{\nabla}\cdot(D\boldsymbol{\nabla}C) = f, \ x \in \Omega, \ t > 0, \\ C(x,t) = g, \ x \in \Gamma_{\text{in}}, \ t > 0, \\ (D\boldsymbol{\nabla}C)\cdot\overrightarrow{n}(x,t) = 0, \ x \in \Gamma_{\text{n}} \cup \Gamma_{\text{out}}, \ t > 0, \\ C(x,0) = C_0(x), \ x \in \Omega. \end{cases} \tag{1}$$

For the inflow boundary, we keep the concentration fixed [30, 31].

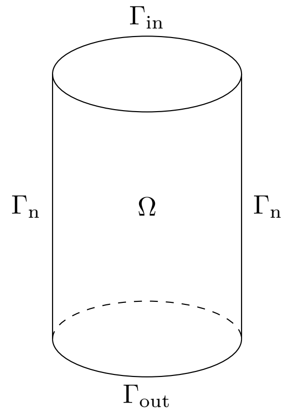

Fig. 1: Schematic of the computational domain Ω and the boundary partition used in the formulation.

We consider three cases of isotherms: (i) constant isotherm, $q(C) = K$, (ii) affine isotherm, $q(C) = K_1 + K_2C$ and (iii) nonlinear, explicit isotherm $q(C)$. A typical example of the nonlinear, explicit isotherm is Langmuir's isotherm [13, 32], $q(C) = \frac{q_{max}K_{eq}C}{1+K_{eq}C}$, where K_{eq} is Langmuir equilibrium constant and q_{max} is the maximum binding capacity of the porous medium. The main result of this paper is second-order accurate by using the symplectic one-step implicit midpoint method for the time discretization, at the same computational cost as the Backward Euler method. The accuracy comes in two ways, such as the rate of convergence is higher and the mass is better conserved when the midpoint method is used. The fully discrete formulation of the problem (1) is given in Section 3. We perform stability analysis and error analysis for the nonlinear explicit $q(C)$ in Section 4. We also prove the existence of a fully discrete solution, and complete the stability analysis and error analysis for the constant and affine $q(C)$ in Section 4. The numerical tests validating these estimates are given in Section 5.

1.1 Previous Work

The general advection–diffusion equation has been the subject of extensive mathematical study during the past decades [33–38]. Recent studies have extended these formulations to model reactive transport with adsorption kinetics relevant to membrane chromatography. In particular, the development of fully implicit stabilized formulations for filtration and separation problems has provided strong theoretical and numerical foundations for analyzing nonlinear adsorption dynamics [39]. Subsequent studies have expanded this framework to incorporate multimodal adsorption isotherms, allowing implicit coupling between the solid- and liquid-phase concentrations and enabling accurate simulation of mixed-mode adsorption under various operating conditions [40]. Experimental investigations have complemented these modeling efforts through the design and characterization of multimodal membrane adsorbers exhibiting high dynamic binding capacities and strong salt tolerance [41], followed by demonstration of effective antibody purification from CHO cell supernatants with high yield and purity using such adsorbers [42]. The mathematical and physical basis of these adsorption models was originally established through detailed analysis of coupled advection–diffusion–reaction equations in functionalized membranes [9]. Convergent linearization methods for nonlinear transport problems are discussed in [43]. Recent numerical analysis for degenerate porous-media transport models (e.g., Richards' equation) includes *a posteriori* error estimation and rigorous convergence/error analyses for finite element, DG, and spectral discretizations [44–46]. The analysis and numerical computations are typically more difficult in the presence of reaction terms, especially nonlinear ones [47]. In [9], the author considered constant, linear, and nonlinear adsorption models and analyzed the problem using the first-order accurate backward Euler method for time discretization and the upwind Petrov–Galerkin (SUPG) finite element method for spatial discretization, with numerical validation for each of the a priori estimates. On the numerical side, the SUPG and related stabilization techniques [48–50] remain the primary tools for advection-dominated transport, while structure-preserving symplectic schemes [51, 52] motivate the second-order midpoint approach used in this paper. A high-order linearly implicit scheme for reaction–diffusion equations was proposed in [53], offering improved temporal accuracy and stability for stiff reactive systems. This approach highlights the importance of efficient time-integration strategies, which also motivates the symplectic midpoint formulation used in the present work. Building upon these prior advances [39–42, 53], the present work extends the stabilized finite-element framework by incorporating a symplectic implicit midpoint time-integration scheme to improve temporal accuracy, ensure mass conservation, and enhance numerical stability for advection-dominated reactive transport problem.

2 Notation and Preliminaries

We denote the $L^2(\Omega)$ norm and inner product by $\|\cdot\|$ and, $(\cdot,\cdot)$ respectively. We denote the usual Sobolev spaces $W^{m,p}(\Omega)$ with the associated norms $\|\cdot\|_{W^{m,p}(\Omega)}$ and in the case when $p=2$, we denote $W^{m,2}(\Omega)=H^m(\Omega)=\{v\in L^2(\Omega): \frac{\partial^\alpha v}{\partial x^\alpha}\in L^2(\Omega),\ |\alpha|\le r\}$

where α is a multi-index, with norm $\|v\|_r = \left(\sum_{|\alpha|\le r} \int_\Omega \left| \frac{\partial^\alpha v}{\partial x^\alpha} \right|^2 d\Omega \right)^{1/2}$. We denote minimum eigenvalue of D as λ. The function space for the liquid phase concentration is defined as:

$$H^1_{0,\Gamma_{\text{in}}}(\Omega) := \{v : v \in H^1(\Omega) \text{ with } v = 0 \text{ on } \Gamma_{\text{in}}\}.$$

Let $X_{0,\Gamma_{\text{in}}} \subset H^1_{0,\Gamma_{\text{in}}}(\Omega)$. We define the space $H^{1/2}(\Gamma_{\text{in}}) := \{g \in L^2(\Gamma_{\text{in}}) : \|g\|_{H^{1/2}(\Gamma_{\text{in}})} < \infty\}$ where

$$\|g\|_{H^{1/2}(\Gamma_{\text{in}})} = \inf_{\substack{G \in H^1(\Omega) \\ G\big|_{\Gamma_{\text{in}}=g}}} \|G\|_{H^1(\Omega)}.$$

The Bochner space [54] norms are

$$\|C\|_{L^2(0,T;X)} = \left(\int_0^T \|C(\cdot,t)\|^2_X dt \right)^{\frac{1}{2}}, \ \|C\|_{L^\infty(0,T;X)} = \text{ess} \sup_{0\le t\le T} \|C(\cdot,t)\|_X.$$

We also define the discrete L^p-norms with $p = 2$ or ∞

$$\|C\|_{L^2(0,T,X)} = \left(\Delta t \sum_{n=0}^{N} \|C^n\|^2_X \right), \quad \|C\|_{L^\infty(0,T,X)} = \max_{0\le n\le N} \|C^n\|_X.$$

For the Finite Element approximation, we consider a regular triangulation of Ω, $\mathcal{T}_h = \{A\}$ with $\Omega = \bigcup_{A\in\mathcal{T}_h} A$. We choose a finite dimensional subspace $X^h \subset H^1(\Omega)$ and define

$$X^h_{0,\Gamma_{\text{in}}} = \{v_h \in X^h : \ v_h = 0 \text{ on } \Gamma_{\text{in}}\}$$

with Ω a polyhedron, $X^h_{0,\Gamma_{\text{in}}} \subset H^1_{0,\Gamma_{\text{in}}}(\Omega)$. Let X^* be the dual space of $X_{0,\Gamma_{\text{in}}}$, with norm $\|f\|_* = \sup_{v\in X_{0,\Gamma_{\text{in}}}} \frac{(f,v)}{\|\nabla v\|}$. We denote $X^h_{\Gamma_{\text{in}}}$ as the restriction of functions in X^h to the boundary Γ_{in} and define $X^h_0 = \{v_h \in X^h : \ v_h = 0 \ on \ \partial\Omega\}$ with Ω a polyhedron, $X^h_0 \subset H^1_0(\Omega)$. Throughout, K will denote a constant taking different values in different instances. We assume that there exists a $k \ge 1$ such that X^h possesses the approximation property,

$$\inf_{C_h\in X^h} \|C - C_h\|_s \le K h^{r-s} \|C\|_r, \text{ for } \ s = 0, 1 \ \text{ and } \ 1 \le r \le k+1. \tag{2}$$

For example, (2) holds if X^h consists of piecewise polynomials of degree $\le k$. We assume that a similar approximation holds on X^h_0. In particular, if $C \in H^r(\Omega) \cap H^1_0(\Omega)$, we will use

$$\inf_{C_h\in X^h_0} \|C - C_h\|_1 \le K h^{r-1} \|C\|_r. \tag{3}$$

We further assume that the space $X^h_{\Gamma_{\rm in}}$ possesses the approximation property

$$\inf_{C_h \in X^h_{\Gamma_{\rm in}}} \|C - C_h\|_{0,\Gamma_{\rm in}} \leq K h^{r-1/2} \|C\|_{r-1/2,\Gamma_{\rm in}}. \tag{4}$$

Lemma 1 *For all $v \in H^1_{0,\Gamma_{in}}(\Omega)$, there exists a constant $\tilde{K}_{PF}$ such that*

$$\|v\|_1 \leq \tilde{K}_{PF} \|\nabla v\|.$$

Proof This is the direct consequence of the Poincaré inequality that holds for $v \in H^1_{0,\Gamma_{\rm in}}(\Omega)$ [55]. □

Lemma 2 *(See [56, p.154]) Let $\mathcal{P}$ and $\mathcal{P}^1$ be the orthogonal projections with respect to the L^2 inner product (u, v) and H^1 inner product $(\nabla u, \nabla v)$, respectively. Then, for any $w \in X$,*

$$\nabla \mathcal{P}_{X^h} w = \mathcal{P}^1_{\nabla X^h} \nabla w.$$

Lemma 3 *Given $g \in H^{r-1/2}(\Gamma_{in})$ for $r \geq 1$, let $\Pi_h g$ denote the $X^h_{\Gamma_{in}}$-interpolant of g. Then, if X^h satisfies the approximation properties (2)-(4),*

$$\inf_{\substack{\hat{C}_h \in X^h \\ \hat{C}_h|_{\Gamma_{in}} = \Pi_h g}} \|C - \hat{C}_h\|_1 \leq K h^{r-1} \|C\|_r. \tag{5}$$

Proof This proof follows the proof of [57, Lemma 4],given here for the reader's convenience. Let $\Pi_h C$ denote X^h-interpolant of C and $\Pi_h g$ denote $X^h_{\Gamma_{\rm in}}$- interpolant of g. Then, for $\hat{C}_h|_{\Gamma_{\rm in}} = \Pi_h g$, we write the triangle inequality

$$\|C - \hat{C}_h\|_1 \leq \|C - \Pi_h C\|_1 + \|\hat{C}_h - \Pi_h C\|_1. \tag{6}$$

From the interpolation theory [58] we get

$$\|C - \Pi_h C\|_1 \leq K h^{r-1} \|C\|_r. \tag{7}$$

We may choose $\hat{C}_h$ so that it has the same value at all interior nodes as does $\Pi_h C$. Since $\hat{C}_h|_{\Gamma_{\rm in}} = \Pi_h g$ and $(\Pi_h C)\Big|_{\Gamma_{\rm in}} = \Pi_h g$, we obtain $(\hat{C}_h - \Pi_h C) = 0$, which concludes the argument. □

2.1 Assumptions and preliminary results

We use the following subset of assumptions considered in [9]:

(F1) ω and ρ_s are constants in time and space [30].
(F2) $\mathbf{u}$ is nonzero and bounded in L^∞ norm [22, 59].
(F3) $D(x) = [d_{ij}]_{i,j=1,2,\cdots,n}$ is symmetric positive definite and $\|D\|_\infty \leq \beta_1$, $|\frac{\partial}{\partial x_i} d_{ij}| \leq \beta_2$, for all i, j [22, 30, 59, 60].
(F4) There exists a unique solution $C \in L^\infty(0, T, L^2(\Omega)) \cap L^2(0, T, H^1(\Omega))$ [22].

(F5) $q = q(C) \in C^1$ is an explicit, Lipschitz continuous function of C, $q(0) = 0$, $q(C) > 0$ for $C > 0$ and $q(C)$ is strictly increasing. Moreover, we assume that $q'(C) \geq \kappa_1 > 0 \;\forall C \geq 0$ [22, 30, 47, 61–63].

(F6) The rate of increase in adsorption is Lipschitz continuous and bounded above so that $\frac{dq}{dC} = q'(C) \leq \kappa_2$ [30].

(F7) The second derivative of the adsorption, $q''(C)$, is Lipschitz continuous and bounded.

Remark 1 *In our analysis we drop the assumption "$C(x,t)$ is nondecreasing in time at every x and $C(x,t) = 0$ on Γ_{in}" stated in [9]. Instead, we consider the non-homogeneous boundary condition at the inflow boundary.*

In [9, 22, 30, 62, 63], another assumption on the continuous and the discrete solution was imposed, namely that "C is non-negative". Using a maximum principle argument, we now prove that the continuous solution is positive and bounded above for all $(x,t) \in \Omega \times (0,T)$.

Proposition 1 *Assuming no forcing term $f = 0$ and the positivity of the initial condition $0 < C_0(x)$, we have that*

$$0 < C(x,t) \leq \max_{x\in\Omega}\{C(x,0), g(x)\} \qquad \textit{for all } (x,t) \in \Omega \times [0,T).$$

Proof From the incompressibility condition, we have

$$\boldsymbol{\nabla}\cdot(\mathbf{u}C) = (\boldsymbol{\nabla}\cdot\mathbf{u})C + \mathbf{u}\cdot\boldsymbol{\nabla}C = \mathbf{u}\cdot\boldsymbol{\nabla}C,$$

If we rewrite the adsorption term as

$$\frac{\partial q}{\partial t} = \frac{\partial q}{\partial C}\frac{\partial C}{\partial t} = q'(C)\frac{\partial C}{\partial t},$$

then the equation (1) becomes

$$(\omega + (1-\omega)\rho_s q'(C))\partial_t C + \mathbf{u}\cdot\boldsymbol{\nabla}C - \boldsymbol{\nabla}\cdot(D\boldsymbol{\nabla}C) = f,\; x \in \Omega,\; t > 0. \tag{8}$$

Since $q'(C) > 0$ by assumption (F5), we can divide (8) by $(\omega + (1-\omega)\rho_s q'(C))$. Hence, assuming $f = 0$, (8) writes,

$$\begin{aligned}&-\partial_t C + \sum_{i,j=1}^{n}\left((\omega + (1-\omega)\rho_s q'(C))^{-1} D_{ij}\right)\frac{\partial^2 C}{\partial x_i \partial x_j}\\ &+ \sum_{j=1}^{n}\left((\omega + (1-\omega)\rho_s q'(C))^{-1}\left(\frac{\partial D_{ij}}{\partial x_i} - u_j\right)\right)\frac{\partial C}{\partial x_j} = 0.\end{aligned}$$

Suppose the claim in the proposition is false. Then there is a $y \in \bar{\Omega}$ and $T > 0$ such that $C(y,T) = 0$ and $C(x,t) > 0$ for $(x,t) \in \bar{\Omega} \times [0,T)$. Therefore, by the Maximum Principle [64, pages 173-174], the maximum of $C(x,t)$ is on the boundary and $(D\boldsymbol{\nabla}C)\cdot\overrightarrow{n}(x,t) < 0$. This contradicts the boundary condition in (1), which concludes the argument. □

3 Variational Formulation

Let $\mathcal{P}$ be the orthogonal projection on $H^1(\Omega)$ with respect to the L^2 inner product (u, v). The standard Galerkin variational formulation for the transport problem (1) is: Find $C \in H^1(\Omega)$ such that $C\Big|_{\Gamma_{\text{in}}} = g$ and

$$\left(\frac{\partial}{\partial t}(\omega C + (1-\omega)\rho_s \mathcal{P}(q(C))), v\right) + (\mathbf{u} \cdot \boldsymbol{\nabla} C, v) + (D\boldsymbol{\nabla} C, \boldsymbol{\nabla} v) = (f, v), \tag{9}$$

for all $v \in H^1_{0,\Gamma_{\text{in}}}(\Omega)$. Next, we write a finite element approximation for (1).

3.1 Semi-Discrete in Space Approximation

Let $\mathcal{P}_h$ be the orthogonal projection on $X^h(\Omega)$ with respect to the L^2 inner product (u, v), and $g_h = \Pi_h g$ an interpolant of g. Then we obtain the following semi-discrete in-space formulation: Find $C_h \in X^h$ such that $C_h\Big|_{\Gamma_{\text{in}}} = g_h$ and $\forall\ v_h \in X^h_{0,\Gamma_{\text{in}}}(\Omega)$,

$$\left(\frac{\partial}{\partial t}(\omega C_h + (1-\omega)\rho_s \mathcal{P}_h(q(C_h))), v_h\right) + (\mathbf{u} \cdot \boldsymbol{\nabla} C_h, v_h) + (D\boldsymbol{\nabla} C_h, \boldsymbol{\nabla} v_h) = (f, v_h). \tag{10}$$

3.2 Fully-discrete approximation

We partition the time interval as $t_0 = 0 < t_1 < t_2 < \cdots < t_N = T$. Let $\Delta t = t_{n+1} - t_n$ be the uniform time step size, $t_n = n\Delta t$, $t_{n+1/2} = \frac{t_n + t_{n+1}}{2}$, and $f^n(x) = f(x, t_n)$. We also denote by $C_h^n(x)$ the Finite Element approximation to $C(x, t_n)$. The midpoint method for time discretization in Finite Element Approximation: Given $C_h^n \in X^h$, find $C_h^{n+1} \in X^h$ such that $C_h^{n+1}\Big|_{\Gamma_{\text{in}}} = g_h$ satisfying

$$\begin{aligned}&\left(\omega\frac{C_h^{n+1} - C_h^n}{\Delta t} + (1-\omega)\rho_s\frac{q(C_h^{n+1}) - q(C_h^n)}{\Delta t}, v_h\right) + (u \cdot \boldsymbol{\nabla} C_h^{n+1/2}, v_h)\\ &+ (D\boldsymbol{\nabla} C_h^{n+1/2}, \boldsymbol{\nabla} v_h) = (f^{n+1/2}, v_h),\ \ \forall v_h \in X^h_{0,\Gamma_{\text{in}}}(\Omega),\end{aligned} \tag{11}$$

where $C_h^{n+\frac{1}{2}}$ denotes $\frac{C_h^n + C_h^{n+1}}{2}$. Equivalently, $\forall v_h \in X^h_{0,\Gamma_{\text{in}}}(\Omega)$,

$$\begin{aligned}&\left((\omega + (1-\omega)\rho_s q'(C_h^{n+1/2}))\frac{C_h^{n+1} - C_h^n}{\Delta t}, v_h\right) + (u \cdot \boldsymbol{\nabla} C_h^{n+1/2}, v_h) + (D\boldsymbol{\nabla} C_h^{n+1/2}, \boldsymbol{\nabla} v_h)\\ &= (f^{n+1/2}, v_h).\end{aligned} \tag{12}$$

To simplify computation, we use the refactorization of the midpoint method [65] for time discretization. Given $C_h^n \in X^h$, find $C_h^{n+1} \in X^h$ such that $C_h^{n+1}\Big|_{\Gamma_{\text{in}}} = g_h$ satisfying

Step 1: Backward Euler method approximating (10) on time interval $[t_n, t_{n+1/2}]$, $\forall\, v_h \in X^h_{0,\Gamma_{\mathrm{in}}}(\Omega)$,

$$\left((\omega + (1-\omega)\rho_s)\frac{q(C_h^{n+1/2}) - q(C_h^n)}{\Delta t/2}, v_h\right) + (\mathbf{u}\cdot\boldsymbol{\nabla} C_h^{n+1/2}, v_h) + (D\boldsymbol{\nabla} C_h^{n+1/2}, \boldsymbol{\nabla} v_h)$$
$$= (f^{n+1/2}, v_h). \tag{13}$$

Step 2: Forward Euler method on time interval $[t_{n+1/2}, t_{n+1}]$, $\forall\, v_h \in X^h_{0,\Gamma_{\mathrm{in}}}(\Omega)$

$$\left((\omega + (1-\omega)\rho_s)\frac{q(C_h^{n+1}) - q(C_h^{n+1/2})}{\Delta t/2}, v_h\right) + (\mathbf{u}\cdot\boldsymbol{\nabla} C_h^{n+1/2}, v_h) + (D\boldsymbol{\nabla} C_h^{n+1/2}, \boldsymbol{\nabla} v_h)$$
$$= (f^{n+1/2}, v_h). \tag{14}$$

Remark 2 *Step 2 is equivalent to a linear extrapolation* $C_h^{n+1} = 2C_h^{n+1/2} - C_h^n$.

3.3 Time-integrated finite element formulation

For the error analysis of the case of a nonlinear, explicit adsorption, we use a time-integrated version of the transport equation introduced in [66] and applied in different formulations [22, 67, 68]. To develop the time-integrated finite element discretization, we rewrite (1) by integrating in time to obtain

$$\omega C + (1-\omega)\rho_s q(C) + \int_0^t \mathbf{u}\cdot\boldsymbol{\nabla} C dt' - \boldsymbol{\nabla}\cdot\int_0^t D\boldsymbol{\nabla} C dt' = \int_0^t f dt' + \omega C_0 + (1-\omega)q(C_0). \tag{15}$$

Testing (15) by $v \in H^1_{0,\Gamma_{in}}(\Omega)$ we get,

$$\begin{aligned}&(\omega C, v) + ((1-\omega)\rho_s q(C), v) + \left(\int_0^t \mathbf{u}\cdot\boldsymbol{\nabla} C dt', v\right) - \left(\boldsymbol{\nabla}\cdot\int_0^t D\boldsymbol{\nabla} C dt', v\right)\\ &= \left(\int_0^t f dt', v\right) + (\omega C_0, v) + ((1-\omega)q(C_0), v).\end{aligned} \tag{16}$$

Then the semi-discrete in space variational formulation is: Find $C_h \in X^h$ such that $C_h\big|_{\Gamma_{in}} = g_h$ and

$$(\omega C_h, v_h) + ((1-\omega)\rho_s q(C_h), v_h) + \left(\int_0^t \mathbf{u}\cdot\boldsymbol{\nabla} C_h dt', v_h\right) - \left(\boldsymbol{\nabla}\cdot\int_0^t D\boldsymbol{\nabla} C_h dt', v_h\right) \tag{17}$$
$$= \left(\int_0^t f dt', v_h\right) + (\omega C_0, v_h) + ((1-\omega)q(C_0), v_h), \quad \forall v_h \in X^h_{0,\Gamma_{in}}(\Omega).$$

Next, the fully discrete variational formulation using the midpoint time discretization can be written as: Given $C_h^n \in X^h$, find $C_h^{n+1} \in X^h$ such that $C_h^{n+1}\big|_{\Gamma_{in}} = g_h$ and

$$\left(\omega C_h^{N+1} + ((1-\omega)\rho_s q(C_h^{N+1}), v_h\right) + \left(\sum_{n=0}^{N} \mathbf{u} \cdot \boldsymbol{\nabla} C_h^{n+1/2}, v_h\right) - \left(\boldsymbol{\nabla} \cdot \sum_{n=0}^{N} D \boldsymbol{\nabla} C_h^{n+1/2}, v_h\right)$$
$$= \left(\sum_{n=0}^{N} f^{n+1/2}, v_h\right) + (\omega C_0, v_h) + ((1-\omega) q(C_0), v_h), \quad \forall v_h \in X_{0,\Gamma_{in}}^h(\Omega). \tag{18}$$

4 Time-Dependent Analysis

In this section, we first construct $\hat{C}$, a continuous extension of the Dirichlet data g inside the domain Ω, to deal with the non-homogeneous boundary condition. Then we perform the stability and error analysis for the time-dependent problem. Detailed proofs of all theorems can be found in [69].

4.1 Construction of $\hat{C}$

Denote $\hat{C}$ as the solution of the following elliptic problem with nonhomogeneous mixed boundary conditions:

$$\begin{aligned} -\boldsymbol{\nabla} \cdot (D \boldsymbol{\nabla} \hat{C}) + \hat{C} &= 0, \ x \in \Omega, \\ \hat{C} &= g, \ \text{if } x \in \Gamma_{\text{in}}, \\ (D \boldsymbol{\nabla} \hat{C}) \cdot \overrightarrow{n} &= 0, \ \text{if } x \in \Gamma_{\text{n}} \cup \Gamma_{\text{out}}. \end{aligned} \tag{19}$$

Lemma 4 *For every $f \in L^2(\Omega)$ and every $g \in H^{1/2}(\Gamma_{in})$, there exists a unique solution $\hat{C} \in H^2(\Omega)$ of (19) under the compatibility condition $D\boldsymbol{\nabla} g \cdot \overrightarrow{n} = 0$ if $x \in \Gamma_{in} \cap \Gamma_n$ such that*

$$\|\hat{C}\|^2 \le 4(K\beta_1)^2 \|g\|^2_{L^2(\Gamma_{in})}, \qquad \|\boldsymbol{\nabla}\hat{C}\|^2 \le \frac{2(K\beta_1)^2}{\lambda}\|g\|^2_{L^2(\Gamma_{in})}. \tag{20}$$

Remark 3 *The existence and uniqueness proof for the more general case of Lemma 4 can be found in [70, Theorem 2.4.2.7].*

Lemma 5 *Let the domain Ω be a convex polyhedral. Given $g^h \in X^h_{\Gamma_{in}}$, there exists a $\hat{C^h} \in X^h$ such that $\hat{C^h}|_{\Gamma-} = g^h$ and $\|\hat{C^h}\|_{H^1(\Omega)} \le K\|g^h\|_{H^{1/2}(\Gamma-)}$.*

Proof When Ω is two-dimensional, we use a similar technique to [71]. Under the compatibility condition $D\boldsymbol{\nabla} g^h \cdot \overrightarrow{n} = 0$, when $x \in \Gamma_{\text{in}} \cap \Gamma_{\text{n}}$, let $\hat{C} \in H^1(\Omega)$ be the solution of

$$\begin{aligned} -\boldsymbol{\nabla} \cdot (D \boldsymbol{\nabla} \hat{C}) + \hat{C} &= 0, \ x \in \Omega, \\ \hat{C} &= g^h, \ \text{when } x \in \Gamma_{\text{in}}, \\ (D \boldsymbol{\nabla} \hat{C}) \cdot \overrightarrow{n} &= 0, \ \text{if } x \in \Gamma_{\text{n}} \cup \Gamma_{\text{out}}. \end{aligned} \tag{21}$$

Since X^h is assumed to be a continuous finite element subspace, we see that g^h is continuous and piecewise smooth along the boundary Γ_{in}, so that $g^h \in H^{1/2+\epsilon}(\Gamma_{\text{in}})$ for $0 < \epsilon \le \frac{1}{2}$. Thus, by elliptic regularity, we derive that $\hat{C} \in H^{1+\epsilon}(\Omega)$ and $\|\hat{C}\|_{1+\epsilon} \le K\|g^h\|_{1/2+\epsilon,\Gamma_{\text{in}}}$ for $0 < \epsilon \le \frac{1}{2}$. Let $\hat{C^h} := \Pi_h \hat{C}$ be the X^h-interpolant of $\hat{C}$ so that $\hat{C^h}|_{\Gamma_{\text{in}}} = g^h$. Then, we have the estimates $\|\hat{C} - \Pi_h\hat{C}\|_1 \le Kh^\epsilon \|\hat{C}\|_{1+\epsilon}$ which can be proven as in, e.g., [72]. Thus, we get

$$\|\hat{C^h}\|_1 = \|\Pi_h\hat{C}\|_1 \le \|\hat{C} - \Pi_h\hat{C}\|_1 + \|\hat{C}\|_1 \le K(h^\epsilon\|\hat{C}\|_{1+\varepsilon} + \|\hat{C}\|_1) \le K\|g^h\|_{1/2,\Gamma_{\text{in}}},$$

where in the last step we used an inverse assumption on $X^h_{\Gamma_{\text{in}}}$: there exists a constant K, independent of h, p^h such that

$$\|p^h\|_{s,\Gamma\text{in}} \le Kh^{t-s}\|p^h\|_{t,\Gamma_{\text{in}}}, \ \forall p^h \in X^h_{\Gamma_{\text{in}}}, \ 0 \le t \le s \le 1.$$

Since the usual interpolant used in the two-dimensional case is not defined in three dimensions for $H^r(\Omega)$-functions, $r \le \frac{3}{2}$, we use the Scott-Zhang interpolant [73] when Ω is three-dimensional. The Scott-Zhang interpolant is well-defined for any function in $H^1(\Omega)$ [74]. □

4.2 Nonlinear, Explicit Isotherm

In this subsection, we start with the numerical analysis for the nonlinear, explicit isotherm. We consider the variational formulation (9), the semi-discrete in-space formulation (10), and the fully discrete formulation given in Section 3.2. First, we show a total mass balance relation for this nonlinear explicit isotherm. We denote the antiderivative of the isotherm by $Q(\alpha) = \int_0^\alpha q(s)ds$, and

$$\begin{aligned}\mathcal{E}(t) = &\frac{3\omega}{4}\int_0^t \left\| D^{1/2}\boldsymbol{\nabla} C - \frac{8}{3}D^{-1/2}\hat{C}\mathbf{u}\right\|^2 dr \\ &+ \frac{3\omega}{4}\int_0^t \left\| D^{1/2}\boldsymbol{\nabla} C - \frac{8\rho_s q(\hat{C})(1-\omega)}{3\omega}D^{-1/2}\mathbf{u}\right\|^2 dr \\ &+ \frac{3\omega}{4}\int_0^t \left\| D^{1/2}\boldsymbol{\nabla} C - \frac{8}{3}D^{-1/2}\boldsymbol{\nabla}\hat{C}\right\|^2 dr \\ &+ \frac{3\omega}{4}\int_0^t \left\| D^{1/2}\boldsymbol{\nabla} C - \frac{8(1-\omega)\rho_s q'(\hat{C})}{3\omega}D^{-1/2}\boldsymbol{\nabla}\hat{C}\right\|^2 dr \\ &+ \|\omega C(t) + (1-\omega)\rho_s q(C(t)) - 2(\omega\hat{C} + (1-\omega)\rho_s q(\hat{C}))\|^2,\end{aligned}$$

also

$$\begin{aligned}\mathcal{B}(t) = &\frac{3\omega}{4}\int_0^t \left\|\frac{8}{3}D^{-1/2}\hat{C}\mathbf{u}\right\|^2 dr + \frac{3\omega}{4}\int_0^t \left\|\frac{8\rho_s q(\hat{C})(1-\omega)}{3\omega}D^{-1/2}\mathbf{u}\right\|^2 dr \\ &+ \frac{3\omega}{4}\int_0^t \left\|\frac{8}{3}D^{-1/2}\boldsymbol{\nabla}\hat{C}\right\|^2 dr + \frac{3\omega}{4}\int_0^t \left\|\frac{8(1-\omega)\rho_s q'(\hat{C})}{3\omega}D^{-1/2}\boldsymbol{\nabla}\hat{C}\right\|^2 dr \\ &+ \|\omega C(0) + (1-\omega)\rho_s q(C(0)) - 2(\omega\hat{C} + (1-\omega)\rho_s q(\hat{C}))\|^2.\end{aligned}$$

Theorem 2 *Assume that (F1)-(F6) are satisfied, $f \in L^2(0,T;L^2(\Omega))$, the variational problem (9) has a solution $C \in L^\infty(0,T,L^2(\Omega)) \cap L^2(0,T,H^1(\Omega))$, and let $\hat{C}$ be solution of (19). Then the following total mass balance relation holds:*

$$
\begin{aligned}
&\|\omega C(t) + (1-\omega)\rho_s q(C(t))\|^2 + \omega \int_0^t \|D^{1/2}\boldsymbol{\nabla} C(r)\|^2\, dr \qquad (22)\\
&\quad + 4(1-\omega)\rho_s \int_0^t \left(\int_\Omega q'(C(r))(D^{1/2}\boldsymbol{\nabla} C(r))^2\, d\Omega + \int_{\Gamma_{out}} Q(C(r))(\mathbf{u}\cdot\overrightarrow{n})ds \right) dr\\
&\quad + 2\omega \int_0^t \left(\int_{\Gamma_{out}} C^2(\mathbf{u}\cdot\overrightarrow{n})ds \right) dr + \mathcal{E}(t)\\
&= \|\omega C_0 + (1-\omega)\rho_s q(C_0)\|^2 + 4\int_0^t (f, \omega C + (1-\omega)\rho_s q(C) - (\omega\hat{C} + (1-\omega)\rho_s q(\hat{C})))\, dr\\
&\quad - 2\omega \int_0^t \left(\int_{\Gamma_{in}} g^2(\mathbf{u}\cdot\overrightarrow{n})ds \right) dr - 4(1-\omega)\rho_s \int_0^t \left(\int_{\Gamma_{in}} Q(g)(\mathbf{u}\cdot\overrightarrow{n})ds \right) dr + \mathcal{B}(t).
\end{aligned}
$$

Proof Let $\hat{C} \in H^1(\Omega)$ such that $\hat{C}\Big|_{\Gamma_{\rm in}} = g$. We test (9) with $v = (\omega C + (1-\omega)\rho_s q(C)) - (\omega\hat{C} + (1-\omega)\rho_s q(\hat{C})) \in H^1_{0,\Gamma_{\rm in}}(\Omega)$. By using the divergence theorem and the boundary conditions, we get

$$
\begin{aligned}
(\mathbf{u}\cdot\boldsymbol{\nabla} C, \omega C + (1-\omega)\rho_s q(C)) &= \frac{\omega}{2}\int_{\Gamma_{\rm in}} g^2(\mathbf{u}\cdot\overrightarrow{n})ds + \frac{\omega}{2}\int_{\Gamma_{\rm out}} C^2(\mathbf{u}\cdot\overrightarrow{n})ds \qquad (23)\\
&+ (1-\omega)\rho_s \int_{\Gamma_{\rm in}} Q(g)(\mathbf{u}\cdot\overrightarrow{n})ds + (1-\omega)\rho_s \int_{\Gamma_{\rm out}} Q(C)(\mathbf{u}\cdot\overrightarrow{n})ds,
\end{aligned}
$$

and

$$
\begin{aligned}
&\omega(D\boldsymbol{\nabla} C, \boldsymbol{\nabla} C) + (1-\omega)\rho_s(q'(C)D\boldsymbol{\nabla} C, \boldsymbol{\nabla} C)\\
&= \omega(D^{1/2}\boldsymbol{\nabla} C, D^{1/2}\boldsymbol{\nabla} C) + (1-\omega)\rho_s(q'(C)D^{1/2}\boldsymbol{\nabla} C, D^{1/2}\boldsymbol{\nabla} C)\\
&= \omega\|D^{1/2}\boldsymbol{\nabla} C\|^2 + (1-\omega)\rho_s \int_\Omega q'(C)(D^{1/2}\boldsymbol{\nabla} C)^2\, d\Omega.
\end{aligned}
$$

Next, we move the terms involving $\hat{C}$ to the right-hand side, and express them as follows

$$
\begin{aligned}
(\mathbf{u}\cdot\boldsymbol{\nabla} C, \omega\hat{C}) &= \frac{3\omega}{8}(D^{1/2}\boldsymbol{\nabla} C, \frac{8}{3}D^{-1/2}\hat{C}\mathbf{u})\\
&= \frac{3\omega}{16}\|D^{1/2}\boldsymbol{\nabla} C\|^2 + \frac{3\omega}{16}\left\|\frac{8}{3}D^{-1/2}\hat{C}\mathbf{u}\right\|^2 - \frac{3\omega}{16}\left\|D^{1/2}\boldsymbol{\nabla} C - \frac{8}{3}D^{-1/2}\hat{C}\mathbf{u}\right\|^2,
\end{aligned}
$$

and

$$
\begin{aligned}
&(\mathbf{u}\cdot\boldsymbol{\nabla} C, (1-\omega)\rho_s q(\hat{C})) = \frac{3\omega}{16}\|D^{1/2}\boldsymbol{\nabla} C\|^2\\
&\quad + \frac{3\omega}{16}\left\|\frac{8\rho_s q(\hat{C})(1-\omega)}{3\omega}D^{-1/2}\mathbf{u}\right\|^2 - \frac{3\omega}{16}\left\|D^{1/2}\boldsymbol{\nabla} C - \frac{8\rho_s q(\hat{C})(1-\omega)}{3\omega}D^{-1/2}\mathbf{u}\right\|^2.
\end{aligned}
$$

Similarly,

$$
\omega(D\boldsymbol{\nabla} C, \boldsymbol{\nabla}\hat{C}) = \frac{3\omega}{16}\|D^{1/2}\boldsymbol{\nabla} C\|^2 + \frac{3\omega}{16}\left\|\frac{8}{3}D^{-1/2}\boldsymbol{\nabla}\hat{C}\right\|^2 - \frac{3\omega}{16}\left\|D^{1/2}\boldsymbol{\nabla} C - \frac{8}{3}D^{-1/2}\boldsymbol{\nabla}\hat{C}\right\|^2,
$$

and

$$(D\nabla C,(1-\omega)\rho_s q'(\hat{C})\nabla\hat{C}) = \frac{3\omega}{16}\|D^{1/2}\nabla C\|^2 + \frac{3\omega}{16}\left\|\frac{8(1-\omega)\rho_s q'(\hat{C})}{3\omega}D^{-1/2}\nabla\hat{C}\right\|^2 - \frac{3\omega}{16}\left\|D^{1/2}\nabla C - \frac{8(1-\omega)\rho_s q'(\hat{C})}{3\omega}D^{-1/2}\nabla\hat{C}\right\|^2.$$

Finally, we express the term involving the time derivative as

$$\left(\frac{\partial}{\partial t}(\omega C+(1-\omega)\rho_s q(C)),\omega\hat{C}+(1-\omega)\rho_s q(\hat{C})\right) = \frac{\partial}{\partial t}(\omega C+(1-\omega)\rho_s q(C),\omega\hat{C}+(1-\omega)\rho_s q(\hat{C})). \tag{24}$$

Combining all, we get,

$$\begin{aligned}
&\frac{1}{2}\frac{\partial}{\partial t}\|\omega C+(1-\omega)\rho_s q(C)\|^2 + \frac{\omega}{4}\|D^{1/2}\nabla C\|^2 + \frac{\omega}{2}\int_{\Gamma_{\text{out}}} C^2(\mathbf{u}\cdot\overrightarrow{n})ds \\
&\quad + (1-\omega)\rho_s\int_{\Gamma_{\text{out}}} Q(C)(\mathbf{u}\cdot\overrightarrow{n})ds + (1-\omega)\rho_s\int_\Omega q'(C)(D^{1/2}\nabla C)^2\,d\Omega \\
&\quad + \frac{3\omega}{16}\left\|D^{1/2}\nabla C - \frac{8}{3}D^{-1/2}\hat{C}\mathbf{u}\right\|^2 + \frac{3\omega}{16}\left\|D^{1/2}\nabla C - \frac{8\rho_s q(\hat{C})(1-\omega)}{3\omega}D^{-1/2}\mathbf{u}\right\|^2 \\
&\quad + \frac{3\omega}{16}\left\|D^{1/2}\nabla C - \frac{8}{3}D^{-1/2}\nabla\hat{C}\right\|^2 + \frac{3\omega}{16}\left\|D^{1/2}\nabla C - \frac{8(1-\omega)\rho_s q'(\hat{C})}{3\omega}D^{-1/2}\nabla\hat{C}\right\|^2 \\
&= (f,\omega C+(1-\omega)\rho_s q(C) - (\omega\hat{C}+(1-\omega)\rho_s q(\hat{C}))) + \frac{3\omega}{16}\left\|\frac{8}{3}D^{-1/2}\hat{C}\mathbf{u}\right\|^2 \\
&\quad + \frac{3\omega}{16}\left\|\frac{8\rho_s q(\hat{C})(1-\omega)}{3\omega}D^{-1/2}\mathbf{u}\right\|^2 + \frac{3\omega}{16}\left\|\frac{8}{3}D^{-1/2}\nabla\hat{C}\right\|^2 + \frac{3\omega}{16}\left\|\frac{8(1-\omega)\rho_s q'(\hat{C})}{3\omega}D^{-1/2}\nabla\hat{C}\right\|^2 \\
&\quad - \frac{\omega}{2}\int_{\Gamma_{\text{in}}} g^2(\mathbf{u}\cdot\overrightarrow{n})ds - (1-\omega)\rho_s\int_{\Gamma_{\text{in}}} Q(g)(\mathbf{u}\cdot\overrightarrow{n})ds \\
&\quad + \frac{\partial}{\partial t}(\omega C+(1-\omega)\rho_s q(C),\omega\hat{C}+(1-\omega)\rho_s q(\hat{C})).
\end{aligned}$$

Integration on $[0,t]$ and the polarized identity yields (22). □

A direct consequence of Theorem 2 is the following stability bound.

Theorem 3 *Assume that (F1)-(F6) are satisfied and the variational formulation given by (9) has a solution $C \in L^\infty(0,T,L^2(\Omega)) \cap L^2(0,T,H^1(\Omega))$ with $f \in L^2(0,T;L^2(\Omega))$. Let $\hat{C}$ be the continuous extension of the Dirichlet data g inside the domain Ω and satisfies (19). The bounds on $\|\hat{C}\|^2$ and $\|\nabla\hat{C}\|^2$ are given in (20). Let the antiderivative be $A(C)=\int_0^C sq'(s)ds$. Then we get the following bound:*

$$\begin{aligned}
&\|C(t)\|^2 + \frac{4}{\omega}\int_\Omega(1-\omega)\rho_s A(C(t))d\Omega + \frac{\lambda}{\omega}\int_0^t\|\nabla C(r)\|^2\,dr + \frac{2}{\omega}\int_0^t\left(\int_{\Gamma_{out}}((C)^2)(\mathbf{u}\cdot\overrightarrow{n})ds\right)dr \\
&\le \frac{4}{\omega}\int_0^t\frac{\|\mathbf{u}\|_\infty^2}{\lambda}\|\hat{C}\|^2\,dr + \left(\frac{\lambda}{\omega}+\frac{4\beta_1^2}{\lambda\omega}\right)\int_0^t\|\nabla\hat{C}\|^2\,dr - \frac{2}{\omega}\int_0^t\left(\int_{\Gamma_{in}}((g)^2)(\mathbf{u}\cdot\overrightarrow{n})ds\right)dr \\
&\quad + 3\|C(0)\|^2 + \frac{8K_{PF}^2}{\lambda\omega}\int_0^t\|f\|^2\,dr + \frac{16(\omega^2+(1-\omega)^2\rho_s^2K^2)}{\omega^2}\|\hat{C}\|^2 \\
&\quad + \frac{4}{\omega}\int_\Omega(1-\omega)\rho_s A(C(0))d\Omega.
\end{aligned}$$

Proof See [69, Theorem 18]. □

Remark 4 *We note that in the case of Langmuir's isotherm, the antiderivative is*

$$A(C(t)) = \ln(1+C) + \frac{1}{1+C} + \text{constant}.$$

Next, we turn to the stability of the semidiscrete in space approximations in (10), and denote:

$$Q_h(\alpha) = \int_0^\alpha \mathcal{P}(q(s))ds,$$

$$\begin{aligned}
\mathcal{E}_h(t) = {} & \frac{3\omega}{4}\int_0^t \left\| D^{1/2}\nabla C_h - \frac{8}{3}D^{-1/2}\hat{C}_h\mathbf{u}\right\|^2 dr + \frac{3\omega}{4}\int_0^t \left\| D^{1/2}\nabla C_h - \frac{8}{3}D^{-1/2}\nabla\hat{C}_h\right\|^2 dr \\
& + \frac{3\omega}{4}\int_0^t \left\| D^{1/2}\nabla C_h - \frac{8\rho_s\mathcal{P}(q(\hat{C}_h))(1-\omega)}{3\omega}D^{-1/2}\mathbf{u}\right\|^2 dr \\
& + \frac{3\omega}{4}\int_0^t \left\| D^{1/2}\nabla C_h - \frac{8(1-\omega)\rho_s\mathcal{P}^1(q'(\hat{C}_h))}{3\omega}D^{-1/2}\nabla\hat{C}_h\right\|^2 dr \\
& + \|\omega C_h(t) + (1-\omega)\rho_s\mathcal{P}(q(C_h(t))) - 2(\omega\hat{C}_h + (1-\omega)\rho_s\mathcal{P}(q(\hat{C}_h)))\|^2,
\end{aligned}$$

and

$$\begin{aligned}
\mathcal{B}_h(t) = {} & \frac{3\omega}{4}\int_0^t \left\| \frac{8}{3}D^{-1/2}\hat{C}\mathbf{u}\right\|^2 dr + \frac{3\omega}{4}\int_0^t \left\| \frac{8\rho_s\mathcal{P}(q(\hat{C}_h))(1-\omega)}{3\omega}D^{-1/2}\mathbf{u}\right\|^2 dr \\
& + \frac{3\omega}{4}\int_0^t \left\| \frac{8}{3}D^{-1/2}\nabla\hat{C}_h\right\|^2 dr + \frac{3\omega}{4}\int_0^t \left\| \frac{8(1-\omega)\rho_s\mathcal{P}^1(q'(\hat{C}))}{3\omega}D^{-1/2}\nabla\hat{C}_h\right\|^2 dr \\
& + \|\omega C(0) + (1-\omega)\rho_s\mathcal{P}(q(C(0))) - 2(\omega\hat{C}_h + (1-\omega)\rho_s\mathcal{P}(q(\hat{C}_h)))\|^2.
\end{aligned}$$

Theorem 4 *Assume that (F1)-(F6) are satisfied, C_h solves the semi-discrete in space Finite Element formulation with nonlinear adsorption* (10), *$f \in L^2(0,T;L^2(\Omega))$, $\hat{C}$ is the solution of (19), $Q_h(\alpha) \geq 0$, and $\mathcal{P}^1(q'(C_h)) \geq 0$. The following total mass balance relation holds:*

$$\begin{aligned}
& \|\omega C_h(t) + (1-\omega)\rho_s\mathcal{P}(q(C_h(t)))\|^2 + \omega\int_0^t \|D^{1/2}\nabla C_h(r)\|^2 dr \\
& \quad + 4(1-\omega)\rho_s\int_0^t \left(\int_\Omega \mathcal{P}^1(q'(C_h(r)))(D^{1/2}\nabla C_h(r))^2 d\Omega\right) dr \\
& \quad + 4(1-\omega)\rho_s\int_0^t \left(\int_{\Gamma_{out}} Q(C_h(r))(\mathbf{u}\cdot\vec{n})ds\right) dr + 2\omega\int_0^t \left(\int_{\Gamma_{out}} C_h^2(\mathbf{u}\cdot\vec{n})ds\right) dr + \mathcal{E}_h(t) \\
& = \|\omega C(0) + (1-\omega)\rho_s\mathcal{P}(q(C_h(0)))\|^2 + \mathcal{B}_h(t) \\
& \quad + 4\int_0^t (f, \omega C_h + (1-\omega)\rho_s\mathcal{P}(q(C_h)) - (\omega\hat{C}_h + (1-\omega)\rho_s\mathcal{P}(q(\hat{C}_h))))\, dr \\
& \quad - 2\omega\int_0^t \left(\int_{\Gamma_{in}} g_h^2(\mathbf{u}\cdot\vec{n})ds\right) dr - 4(1-\omega)\rho_s\int_0^t \left(\int_{\Gamma_{in}} Q(g_h)(\mathbf{u}\cdot\vec{n})ds\right) dr.
\end{aligned}$$

Proof Let $\hat{C}_h \in X^h(\Omega)$ such that $\hat{C}_h\Big|_{\Gamma_{\text{in}}} = g_h$ be the interpolant given in Lemma 5, and $\mathcal{P}$, $\mathcal{P}^1$ be the orthogonal projections with respect to the L^2 and H^1 inner products , respectively. Then we test (10) with $v_h = (\omega C_h + (1-\omega)\rho_s\mathcal{P}(q(C_h))) - (\omega\hat{C}_h + (1-\omega)\rho_s\mathcal{P}(q(\hat{C}_h))) \in X^h_{0,\Gamma_{\text{in}}}(\Omega)$ to obtain

$$\begin{aligned}
&\left(\frac{\partial}{\partial t}(\omega C_h + (1-\omega)\rho_s q(C_h)), \omega C_h + (1-\omega)\rho_s\mathcal{P}(q(C_h))\right) + \omega(D\boldsymbol{\nabla} C_h, \boldsymbol{\nabla} C_h) \qquad (25)\\
&\quad + \left(\mathbf{u}\cdot\boldsymbol{\nabla} C_h, \omega C_h + (1-\omega)\rho_s\mathcal{P}(q(C_h))\right) + (1-\omega)\rho_s(D\boldsymbol{\nabla} C_h, \mathcal{P}^1(q'(C_h)\boldsymbol{\nabla} C_h))\\
&= (f, \omega C_h + (1-\omega)\rho_s\mathcal{P}(q(C_h)) - (\omega\hat{C}_h + (1-\omega)\rho_s\mathcal{P}(q(\hat{C}_h))))\\
&\quad + \left(\frac{\partial}{\partial t}(\omega C_h + (1-\omega)\rho_s q(C_h)), (\omega\hat{C}_h + (1-\omega)\rho_s\mathcal{P}(q(\hat{C}_h)))\right) + \omega(D\boldsymbol{\nabla} C_h, \boldsymbol{\nabla}\hat{C}_h)\\
&\quad + \left(\mathbf{u}\cdot\boldsymbol{\nabla} C, (\omega\hat{C}_h + (1-\omega)\rho_s\mathcal{P}(q(\hat{C}_h)))\right) + (1-\omega)\rho_s(D\boldsymbol{\nabla} C_h, \mathcal{P}^1(q'(\hat{C}_h)\boldsymbol{\nabla}\hat{C}_h)).
\end{aligned}$$

We rewrite the first term in the left hand side as

$$\left(\frac{\partial}{\partial t}(\omega C_h + (1-\omega)\rho_s q(C_h)), \omega C_h + (1-\omega)\rho_s\mathcal{P}(q(C_h))\right) = \frac{1}{2}\frac{\partial}{\partial t}\|\omega C_h + (1-\omega)\rho_s\mathcal{P}(q(C_h))\|^2. \qquad (26)$$

Following the technique used in Theorem 2 we get

$$\begin{aligned}
&(\mathbf{u}\cdot\boldsymbol{\nabla} C_h, \omega C_h + (1-\omega)\rho_s\mathcal{P}(q(C_h))) \qquad (27)\\
&= \frac{\omega}{2}\int_{\Gamma_{\text{in}}} g_h^2(\mathbf{u}\cdot\overrightarrow{n})ds + \frac{\omega}{2}\int_{\Gamma_{\text{out}}} C_h^2(\mathbf{u}\cdot\overrightarrow{n})ds\\
&\quad + (1-\omega)\rho_s\int_{\Gamma_{\text{in}}} Q_h(g_h)(\mathbf{u}\cdot\overrightarrow{n})ds + (1-\omega)\rho_s\int_{\Gamma_{\text{out}}} Q_h(C_h)(\mathbf{u}\cdot\overrightarrow{n})ds,
\end{aligned}$$

and

$$\begin{aligned}
&\omega(D\boldsymbol{\nabla} C_h, \boldsymbol{\nabla} C_h) + (1-\omega)\rho_s\mathcal{P}^1(q'(C_h)D\boldsymbol{\nabla} C_h, \boldsymbol{\nabla} C_h) \qquad (28)\\
&= \omega\|D^{1/2}\boldsymbol{\nabla} C_h\|^2 + (1-\omega)\rho_s\int_\Omega \mathcal{P}^1(q'(C_h))(D^{1/2}\boldsymbol{\nabla} C_h)^2\ d\Omega.
\end{aligned}$$

Also, the terms on the right-hand side write as

$$(\mathbf{u}\cdot\boldsymbol{\nabla} C_h, \omega\hat{C}_h) = \frac{3\omega}{16}\|D^{1/2}\boldsymbol{\nabla} C_h\|^2 + \frac{3\omega}{16}\left\|\frac{8}{3}D^{-1/2}\hat{C}_h\mathbf{u}\right\|^2 - \frac{3\omega}{16}\left\|D^{1/2}\boldsymbol{\nabla} C_h - \frac{8}{3}D^{-1/2}\hat{C}_h\mathbf{u}\right\|^2, \qquad (29)$$

and

$$\begin{aligned}
(\mathbf{u}\cdot\boldsymbol{\nabla} C_h, (1-\omega)\rho_s\mathcal{P}(q(\hat{C}_h))) &= \frac{3\omega}{16}\|D^{1/2}\boldsymbol{\nabla} C_h\|^2 + \frac{3\omega}{16}\left\|\frac{8\rho_s\mathcal{P}(q(\hat{C}_h))(1-\omega)}{3\omega}D^{-1/2}\mathbf{u}\right\|^2\\
&\quad - \frac{3\omega}{16}\left\|D^{1/2}\boldsymbol{\nabla} C_h - \frac{8\rho_s\mathcal{P}(q(\hat{C}_h))(1-\omega)}{3\omega}D^{-1/2}\mathbf{u}\right\|^2.
\end{aligned}$$

Moreover,

$$\begin{aligned}
&\omega(D\boldsymbol{\nabla} C_h, \boldsymbol{\nabla}\hat{C}_h) \qquad (30)\\
&= \frac{3\omega}{16}\|D^{1/2}\boldsymbol{\nabla} C_h\|^2 + \frac{3\omega}{16}\left\|\frac{8}{3}D^{-1/2}\boldsymbol{\nabla}\hat{C}_h\right\|^2 - \frac{3\omega}{16}\left\|D^{1/2}\boldsymbol{\nabla} C_h - \frac{8}{3}D^{-1/2}\boldsymbol{\nabla}\hat{C}_h\right\|^2,
\end{aligned}$$

$$(D\boldsymbol{\nabla}C_h,(1-\omega)\rho_s\mathcal{P}^1(q'(\hat{C}_h))\boldsymbol{\nabla}\hat{C}_h) \tag{31}$$
$$=\frac{3\omega}{16}\|D^{1/2}\boldsymbol{\nabla}C_h\|^2+\frac{3\omega}{16}\left\|\frac{8(1-\omega)\rho_s\mathcal{P}^1(q'(\hat{C}_h))}{3\omega}D^{-1/2}\boldsymbol{\nabla}\hat{C}_h\right\|^2$$
$$-\frac{3\omega}{16}\left\|D^{1/2}\boldsymbol{\nabla}C_h-\frac{8(1-\omega)\rho_s\mathcal{P}^1(q'(\hat{C}_h))}{3\omega}D^{-1/2}\boldsymbol{\nabla}\hat{C}_h\right\|^2,$$

and

$$\left(\frac{\partial}{\partial t}(\omega C_h+(1-\omega)\rho_s q(C_h)),\omega\hat{C}_h+(1-\omega)\rho_s\mathcal{P}(q(\hat{C}_h))\right) \tag{32}$$
$$=\frac{\partial}{\partial t}(\omega C_h+(1-\omega)\rho_s q(C_h),\omega\hat{C}_h+(1-\omega)\rho_s\mathcal{P}(q(\hat{C}_h))).$$

Combining (26)-(32) and integrating both sides from 0 to t, we obtain

$$\frac{1}{2}\|\omega C_h(t)+(1-\omega)\rho_s\mathcal{P}(q(C(t)))\|^2+\frac{\omega}{4}\int_0^t\|\boldsymbol{\nabla}C_h(r)\|^2\,dr+\frac{\omega}{2}\int_0^t\left(\int_{\Gamma_{\mathrm{out}}}C_h^2(\mathbf{u}\cdot\overrightarrow{n})ds\right)dr$$
$$+(1-\omega)\rho_s\int_0^t\int_{\Gamma_{\mathrm{out}}}Q_h(C_h(r))(\mathbf{u}\cdot\overrightarrow{n})ds\,dr+\frac{3\omega}{16}\int_0^t\left\|D^{1/2}\boldsymbol{\nabla}C_h(r)-\frac{8}{3}D^{-1/2}\hat{C}_h\mathbf{u}\right\|^2dr$$
$$+(1-\omega)\rho_s\int_0^t\int_\Omega\mathcal{P}^1(q'(C_h(r)))(D^{1/2}\boldsymbol{\nabla}C_h(r))^2\,d\Omega\,dr$$
$$+\frac{3\omega}{16}\int_0^t\left\|D^{1/2}\boldsymbol{\nabla}C_h(r)-\frac{8\rho_s\mathcal{P}(q(\hat{C}_h))(1-\omega)}{3\omega}D^{-1/2}\mathbf{u}\right\|^2dr$$
$$+\frac{3\omega}{16}\int_0^t\left\|D^{1/2}\boldsymbol{\nabla}C_h(r)-\frac{8}{3}D^{-1/2}\boldsymbol{\nabla}\hat{C}_h\right\|^2dr$$
$$+\frac{3\omega}{16}\int_0^t\left\|D^{1/2}\boldsymbol{\nabla}C_h(r)-\frac{8(1-\omega)\rho_s\mathcal{P}^1(q'(\hat{C}_h))}{3\omega}D^{-1/2}\boldsymbol{\nabla}\hat{C}_h\right\|^2dr$$
$$=\int_0^t(f,\omega C_h+(1-\omega)\rho_s\mathcal{P}(q(C_h))-(\omega\hat{C}_h+(1-\omega)\rho_s\mathcal{P}(q(\hat{C}_h))))\,dr+\frac{3\omega}{16}\int_0^t\left\|\frac{8}{3}D^{-1/2}\hat{C}_h\mathbf{u}\right\|^2dr$$
$$+\frac{3\omega}{16}\int_0^t\left\|\frac{8\rho_s\mathcal{P}(q(\hat{C}_h))(1-\omega)}{3\omega}D^{-1/2}\mathbf{u}\right\|^2dr+\frac{3\omega}{16}\int_0^t\left\|\frac{8}{3}D^{-1/2}\boldsymbol{\nabla}\hat{C}_h\right\|^2dr$$
$$+\frac{3\omega}{16}\int_0^t\left\|\frac{8(1-\omega)\rho_s\mathcal{P}^1(q'(\hat{C}_h))}{3\omega}D^{-1/2}\boldsymbol{\nabla}\hat{C}_h\right\|^2dr+\frac{1}{2}\|\omega C_h(0)+(1-\omega)\rho_s\mathcal{P}(q(C_h(0)))\|^2$$
$$-\frac{\omega}{2}\int_0^t\left(\int_{\Gamma_{\mathrm{in}}}g_h^2(\mathbf{u}\cdot\overrightarrow{n})ds\right)dr-(1-\omega)\rho_s\int_0^t\left(\int_{\Gamma_{\mathrm{in}}}Q_h(g_h)(\mathbf{u}\cdot\overrightarrow{n})ds\right)dr$$
$$+(\omega C_h(t)+(1-\omega)\rho_s q(C_h(t)),\omega\hat{C}_h+(1-\omega)\rho_s\mathcal{P}(q(\hat{C}_h)))$$
$$-(\omega C_h(0)+(1-\omega)\rho_s q(C_h(0)),\omega\hat{C}_h+(1-\omega)\rho_s\mathcal{P}(q(\hat{C}_h))).$$

Writing the last two terms as

$$(\omega C_h(t)+(1-\omega)\rho_s q(C_h(t)),\omega\hat{C}_h+(1-\omega)\rho_s\mathcal{P}(q(\hat{C}_h)))$$
$$=\frac{1}{4}\|(\omega C_h(t)+(1-\omega)\rho_s q(C_h(t))\|^2+\frac{1}{4}\|2(\omega\hat{C}_h+(1-\omega)\rho_s\mathcal{P}(q(\hat{C}_h)))\|^2$$
$$-\frac{1}{4}\|\omega C_h(t)+(1-\omega)\rho_s q(C_h(t))-2(\omega\hat{C}_h+(1-\omega)\rho_s\mathcal{P}(q(\hat{C}_h)))\|^2,$$

and

$$-(\omega C_h(0)+(1-\omega)\rho_s q(C_h0)),\omega\hat{C}_h+(1-\omega)\rho_s\mathcal{P}(q(\hat{C}_h)))$$

$$= -\frac{1}{4}\|(\omega C_h(0) + (1-\omega)\rho_s q(C_h(0))\|^2 - \frac{1}{4}\|2(\omega\hat{C}_h + (1-\omega)\rho_s \mathcal{P}(q(\hat{C}_h)))\|^2$$
$$+ \frac{1}{4}\|\omega C_h(0) + (1-\omega)\rho_s q(C_h(0)) - 2(\omega\hat{C}_h + (1-\omega)\rho_s\mathcal{P}(q(\hat{C}_h)))\|^2,$$

yields the claimed result. □

4.2.1 Semi-discrete in space error estimate

The following result gives an a priori error estimate of the semi-discrete in space approximation (17) for the case of nonlinear adsorption.

Theorem 5 *Assume that (F1)-(F7) are satisfied, the variational formulation* (16) *with nonlinear adsorption has an exact solution* $C \in H^1(0,T,H^{k+1}(\Omega))$*, and* C_h *solves the semi-discrete in space Finite Element formulation* (17)*. Then for all* $1 \le r \le k+1$ *and each* $T > 0$ *we have*

$$\omega\int_0^T \|(C-C_h)\|^2 dt + \|\int_0^T D^{1/2}\boldsymbol{\nabla}(C-C_h)dt'\|^2 \le h^{2r-2}\int_0^T \|C\|_r^2 dt \tag{33}$$
$$\times \exp\left(T + \frac{3T\|u\|_\infty^2\|D^{-1/2}\|_\infty^2}{\omega}\right)\left(4\|D^{1/2}\|_\infty^2 + 3\omega + 4\|u\|_\infty^2\|D^{-1/2}\|_\infty^2 + \frac{3(1-\omega)^2\rho_s^2\kappa_2^2}{\omega}\right)K^2.$$

Proof Let $v = v_h \in X^h_{0,\Gamma_{\text{in}}} \subset H^1_{0,\Gamma_{\text{in}}}(\Omega)$ in (16), and then subtract (17) from (16) to obtain

$$0 = (\omega(C-C_h), v_h) + ((1-\omega)\rho_s(q(C)-q(C_h)), v_h) + \left(\int_0^t u\cdot\boldsymbol{\nabla}(C-C_h)dt', v_h\right) \tag{34}$$
$$- (\boldsymbol{\nabla}\cdot\int_0^t D\boldsymbol{\nabla}(C-C_h)dt', v_h), \quad \forall v_h \in X^h_{0,\Gamma_{in}}(\Omega).$$

Choosing $v_h = C_h - \hat{C}_h = C_h - C + C - \hat{C}_h \in X^h_{0,\Gamma_{\text{in}}}$ gives

$$(\omega(C-C_h), C-C_h) + ((1-\omega)\rho_s(q(C)-q(C_h)), C-C_h)$$
$$+ \left(\int_0^t u\cdot\boldsymbol{\nabla}(C-C_h)dt', C-C_h\right) + \left(\int_0^t D\boldsymbol{\nabla}(C-C_h)dt', \boldsymbol{\nabla}(C-C_h)\right)$$
$$= (\omega(C-C_h), C-\hat{C}_h) + ((1-\omega)\rho_s(q(C)-q(C_h)), C-\hat{C}_h)$$
$$+ \left(\int_0^t u\cdot\boldsymbol{\nabla}(C-C_h)dt', C-\hat{C}_h\right) + \left(\int_0^t D\boldsymbol{\nabla}(C-C_h)dt', \boldsymbol{\nabla}\left(C-\hat{C}_h\right)\right).$$

The Cauchy-Schwarz inequality and integration on $[0,T]$ yields

$$\omega\int_0^T \|C-C_h\|^2 dt + 2(1-\omega)\rho_s\int_0^T\int_\Omega\left(\int_0^1 (q'(\theta C + (1-\theta)C_h))d\theta\right)(C-C_h)^2 d\Omega\, dt$$
$$+ \left\|\int_0^T D^{1/2}\boldsymbol{\nabla}(C-C_h)dt'\right\|^2$$
$$\le \left(1 + \frac{3\|u\|_\infty^2\|D^{-1/2}\|_\infty^2}{\omega}\right)\int_0^T \|\int_0^t D^{1/2}\boldsymbol{\nabla}(C-C_h)dt'\|^2 dt + 4\|D^{1/2}\|_\infty^2\int_0^T \|\boldsymbol{\nabla}\left(C-\hat{C}_h\right)\|^2 dt$$
$$+ \left(3\omega + 4\|u\|_\infty^2\|D^{-1/2}\|_\infty^2 + \frac{3(1-\omega)^2\rho_s^2\kappa_2^2}{\omega}\right)\int_0^T \|C-\hat{C}_h\|^2 dt.$$

Discarding the second term in the left hand side and using the Gronwall's inequality gives

$$
\begin{aligned}
&\omega \int_0^T \|(C - C_h)\|^2 dt + \left\| \int_0^T D^{1/2}\boldsymbol{\nabla}(C - C_h)dt' \right\|^2 \\
&\leq \exp\left(T + \frac{3T\|u\|_\infty^2 \|D^{-1/2}\|_\infty^2}{\omega}\right) \\
&\quad \times \left(4\|D^{1/2}\|_\infty^2 + +3\omega + 4\|u\|_\infty^2\|D^{-1/2}\|_\infty^2 + \frac{3(1-\omega)^2\rho_s^2\kappa_2^2}{\omega}\right) \int_0^T \inf_{\substack{\hat{C_h} \in X^h \\ \hat{C_h}|_{\Gamma_{\rm in}} = g_h}} \|C - \hat{C}_h\|_1^2 dt.
\end{aligned}
$$

Let boundary term g_h be the interpolant of g in $X_{\Gamma_{\rm in}}^h$. Then Lemma 3 finally implies (33). $\square$

4.2.2 Existence of the solution to the fully discrete system

In this subsection, we prove the solvability of the fully discrete system (12), approximating (1) for the nonlinear explicit isotherm. By adding and subtracting $\hat{C}_h$ and multiplying by 2, we rewrite (12) as follows: Given $C_h^n - \hat{C}_h \in X_{0,\Gamma_{\rm in}}^h$, find $C_h^{n+1} - \hat{C}_h \in X_{0,\Gamma_{\rm in}}^h$ such that

$$
\begin{aligned}
&(D\nabla(C_h^{n+1} - \hat{C}_h), \nabla v_h) \\
&= -2\left(\left(\omega + (1-\omega)\rho_s q'(\frac{C_h^{n+1} - \hat{C}_h + C_h^n + \hat{C}_h}{2})\right) \frac{(C_h^{n+1} - \hat{C}_h) - (C_h^n - \hat{C}_h)}{\Delta t}, v_h\right) \\
&+ 2(f^{n+1/2}, v_h) - (\mathbf{u} \cdot \nabla(C_h^{n+1} - \hat{C}_h + C_h^n + \hat{C}_h), v_h) + (\nabla \cdot (D\nabla(C_h^n + \hat{C}_h)), v_h),
\end{aligned} \tag{35}
$$

for all $v_h \in X_{0,\Gamma_{\rm in}}^h$. To simplify the presentation, we drop the subscript h throughout this section. We note that by the Lax-Milgram theorem [75, corollary 5.8] we have that

$\forall\, l \in X^*$, there exists an unique solution $\Psi \in X_{0,\Gamma_{\rm in}}$ of $(D\boldsymbol{\nabla}\Psi, \boldsymbol{\nabla}v) = (l, v)$, $\forall v \in X_{0,\Gamma_{\rm in}}$,

and therefore, the operator $T : X^* \to X_{0,\Gamma_{\rm in}}$ defined by $T(l) = \Psi$ is a well-defined linear and continuous operator:

$$
\|T\| = \sup_{l \in X^*} \frac{\|T(l)\|_{X_{0,\Gamma_{\rm in}}}}{\|l\|_*} = \sup_{l \in X^*} \frac{\|\boldsymbol{\nabla}\Psi\|}{\|l\|_*} \leq \frac{1}{\lambda}, \text{ since } \|\boldsymbol{\nabla}\Psi\| \leq \frac{1}{\lambda}\|l\|_*.
$$

Next, we define the nonlinear operator $N : X_{0,\Gamma_{\rm in}} \to X^*$ by

$$
\begin{aligned}
N(\psi) = 2f^{n+\frac{1}{2}} - 2\left(\omega + (1-\omega)\rho_s q'\left(\frac{\psi + C^n + \hat{C}}{2}\right)\right) \frac{\psi - (C^n - \hat{C})}{\Delta t} - \mathbf{u} \cdot \nabla(\psi + C^n + \hat{C}) \\
+ \boldsymbol{\nabla} \cdot (D\nabla(C^n + \hat{C})),
\end{aligned}
$$

and the operator $\mathcal{F} : X_{0,\Gamma_{\rm in}} \to X_{0,\Gamma_{\rm in}}$ by $\mathcal{F} = T(N(\psi))$. To prove the solvability of the problem (35), it suffices to show that $\mathcal{F}$ has a fixed point, i.e., there exists $\psi = \mathcal{F}(\psi) \in X_{0,\Gamma_{\rm in}}$.

Lemma 6 *$N : X_{0,\Gamma_{in}} \to X^*$ is a bounded operator*

$$\|N(\psi)\|_* \leq \|\mathbf{u}\|_\infty \|\boldsymbol{\nabla}\psi\| + \frac{2\omega + 2(1-\omega)\kappa_2}{\Delta t}\|\psi\| + \frac{2\omega + 2(1-\omega)\kappa_2}{\Delta t}\|C^n - \hat{C}\| + \|2f^{n+\frac{1}{2}}\|_* + \|\boldsymbol{\nabla} \cdot (D\nabla(C^n + \hat{C}))\|_* + \|\mathbf{u}\|_\infty \|\nabla(C^n + \hat{C})\|.$$

Remark 5 *The proof of Lemma 6 follows from (F6), the triangle and Cauchy-Schwarz inequalities.*

Lemma 7 *$N : X_{0,\Gamma_{in}} \to X^*$ is a continuous operator.*

Proof It suffices to show that $\|N(\psi_1) - N(\psi_2)\|_* \to 0$ if $\|\boldsymbol{\nabla}(\psi_1 - \psi_2)\| \to 0$ because $\|\psi\|_{X_{0,\Gamma_{\rm in}}}$ is equivalent to $\|\boldsymbol{\nabla}\psi\|$. Here,

$$\begin{aligned}
&\|N(\psi_1) - N(\psi_2)\|_* \\
&\leq \frac{2\omega}{\Delta t}\|\psi_2 - \psi_1\|_* + \|\mathbf{u} \cdot \boldsymbol{\nabla}(\psi_2 - \psi_1)\|_* \\
&+ \frac{2(1-\omega)\rho_s}{\Delta t}\|q'(\frac{\psi_2 + C^n + \hat{C}}{2})(\psi_2 - (C^n - \hat{C})) - q'(\frac{\psi_1 + C^n + \hat{C}}{2})(\psi_1 - (C^n - \hat{C}))\|_*.
\end{aligned}$$

Notice, $\frac{2\omega}{\Delta t}\|\psi_2 - \psi_1\|_* \leq \frac{2\omega K_{\rm PF}}{\Delta t}\|\boldsymbol{\nabla}(\psi_2 - \psi_1)\|$ and $\|\mathbf{u} \cdot \boldsymbol{\nabla}(\psi_2 - \psi_1)\|_* \leq \|\mathbf{u}\|_\infty \|\boldsymbol{\nabla}(\psi_2 - \psi_1)\|$. Next,

$$\|q'(\frac{\psi_2 + C^n + \hat{C}}{2})(\psi_2 - \psi_1)\|_* \leq \kappa_2 K_{\rm PF}\|\boldsymbol{\nabla}(\psi_2 - \psi_1)\|.$$

Using Lipschitz continuity of q' we get,

$$\begin{aligned}
&\|\left(q'(\frac{\psi_2 + C^n + \hat{C}}{2}) - q'(\frac{\psi_1 + C^n + \hat{C}}{2})\right)(\psi_1 - (C^n - \hat{C}))\|_* \\
&\leq K K_{\rm PF}\|\boldsymbol{\nabla}(\psi_2 - \psi_1)\|\|\psi_1 - (C^n - \hat{C})\|.
\end{aligned}$$

Hence, using Cauchy-Schwarz, Poincaré-Friedrichs inequalities and Lipschitz continuity of q' we get,

$$\begin{aligned}
&\|N(\psi_1) - N(\psi_2)\|_* \\
&\leq \left(\frac{2\omega K_{\rm PF}}{\Delta t} + \|\mathbf{u}\|_\infty + \frac{2(1-\omega)\rho_s\kappa_2 K_{\rm PF}}{\Delta t} + \frac{2(1-\omega)\rho_s K K_{\rm PF}}{\Delta t}\|\psi_1 - (C^n - \hat{C})\|\right) \\
&\times \|\boldsymbol{\nabla}(\psi_2 - \psi_1)\|
\end{aligned}$$

which concludes the argument. □

Lemma 8 *$\mathcal{F} : X_{0,\Gamma_{in}} \to X_{0,\Gamma_{in}}$ is a compact map.*

Proof Since $T : X^* \to X_{0,\Gamma_{\rm in}}$ is a bounded linear operator, we only need to show that $N : X_{0,\Gamma_{\rm in}} \to X^*$ is a compact map. By Lemmas 6-7 we have that $N : X_{0,\Gamma_{\rm in}} \to X^*$ is a bounded and continuous operator respectively, and the Rellich-Kondrachov theorem [76, page 272] provides the compact embedding $I : X_{0,\Gamma_{\text{in}}} \hookrightarrow L^2$ defined by $I(\psi) = \psi$. Therefore $N \circ I : X_{0,\Gamma_{\text{in}}} \hookrightarrow L^2 \to X^*$ is compact.

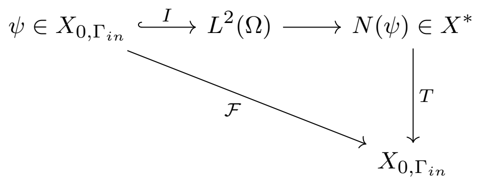

□

Theorem 6 *For any $v \in X_{0,\Gamma_{in}}$ and $f \in X^*$, there exists $\psi = C^{n+1} - \hat{C} \in X_{0,\Gamma_{in}}$ solution to eq. (35).*

Proof Consider $\psi_\alpha = \alpha \mathcal{F}(\psi_\alpha)$ in $X_{0,\Gamma_{\text{in}}}$, $0 \le \alpha \le 1$ defined by

$$\psi_\alpha = T\Big(2\alpha f^{n+\frac{1}{2}} - 2\alpha\Big(\omega + (1-\omega)\rho_s q'(\frac{\psi + C^n + \hat{C}}{2})\Big)\frac{\psi - (C^n - \hat{C})}{\Delta t} \\ - \alpha \mathbf{u} \cdot \nabla(\psi + C^n + \hat{C}) + \alpha \boldsymbol{\nabla} \cdot (D\nabla(C^n + \hat{C}))\Big),$$

which holds if and only if for all $v \in X_{0,\Gamma_{\text{in}}}$ $\psi_\alpha \in X_{0,\Gamma_{\text{in}}}$ satisfies

$$(D\boldsymbol{\nabla}\psi_\alpha, \boldsymbol{\nabla} v) = -2\alpha\Big(\Big(\omega + (1-\omega)\rho_s q'(\frac{\psi_\alpha + C^n + \hat{C}}{2})\Big)\frac{\psi_\alpha - (C^n - \hat{C})}{\Delta t}, v\Big) \\ + 2(\alpha f^{n+1/2}, v) - (\alpha \mathbf{u} \cdot \boldsymbol{\nabla}\Big(\psi_\alpha + C^n + \hat{C}\Big), v) - (\alpha D \boldsymbol{\nabla}\Big(C^n + \hat{C}\Big), \boldsymbol{\nabla} v).$$

Then, by the Leray-Schauder fixed-point theorem [77, 78], we only need to prove an a priori bound on $\|\boldsymbol{\nabla}\psi_\alpha\|$, independent of α. This follows by setting $v = \psi_\alpha$ and using the Cauchy-Schwarz and Poincaré-Friedrichs inequalities

$$\|\boldsymbol{\nabla}\psi_\alpha\| \le \frac{2K_{\text{PF}}}{\lambda}\|f^{n+1/2}\| + \frac{K_{\text{PF}}}{\lambda}\|\mathbf{u} \cdot \nabla(C^n + \hat{C})\| + \frac{\beta_1}{\lambda}\|\nabla(C^n + \hat{C})\| \\ + \frac{2K_{\text{PF}}(\omega + (1-\omega)\rho_s \kappa_2)}{\lambda \Delta t}\|C^n - \hat{C}\|, \text{ for } 0 \le \alpha \le 1.$$

□

4.2.3 Stability of the solution to the fully discrete system

In this subsection, we derive an energy-like bound for (13)-(14), the fully discrete version of the adsorption equation (1) for a nonlinear, explicit isotherm, using the midpoint method for the time discretization. We recall that at the continuous level, we proved that the solution $C > 0$ is positive, and it is bounded by the initial and boundary conditions. Nevertheless, positivity at the discrete level and a discrete Maximum Principle are hard to obtain and usually hold under a CFL condition, i.e., the timestep has to be $\mathcal{O}(h^2)$ [79]. We use the following notations: $Q_h(\alpha) = \int_0^\alpha \mathcal{P}(q(s))ds$,

$$\mathcal{E}_h^n = \frac{3\Delta t \omega}{4}\sum_{n=0}^{N}\left\| D^{1/2}\boldsymbol{\nabla} C_h^{n+1/2} - \frac{8}{3}D^{-1/2}\hat{C}_h \mathbf{u}\right\|^2$$

$$+\frac{3\Delta t\omega}{4}\sum_{n=0}^{N}\left\|D^{1/2}\boldsymbol{\nabla}C_h^{n+1/2}-\frac{8\rho_s\mathcal{P}(q(\hat{C}_h))(1-\omega)}{3\omega}D^{-1/2}\mathbf{u}\right\|^2$$
$$+\frac{3\Delta t\omega}{4}\sum_{n=0}^{N}\left\|D^{1/2}\boldsymbol{\nabla}C_h^{n+1/2}-\frac{8}{3}D^{-1/2}\boldsymbol{\nabla}\hat{C}_h\right\|^2$$
$$+\frac{3\Delta t\omega}{4}\sum_{n=0}^{N}\left\|D^{1/2}\boldsymbol{\nabla}C_h^{n+1/2}-\frac{8(1-\omega)\rho_s\mathcal{P}^1(q'(\hat{C}_h))}{3\omega}D^{-1/2}\boldsymbol{\nabla}\hat{C}_h\right\|^2$$
$$+\|\omega C_h^{N+1}+(1-\omega)\rho_s q(C_h^{N+1})-2(\omega\hat{C}_h+(1-\omega)\rho_s\mathcal{P}(q(\hat{C}_h)))\|^2,$$

and

$$\begin{aligned}\mathcal{B}_h^n=&\frac{3N\Delta t\omega}{4}\left\|\frac{8}{3}D^{-1/2}\hat{C}_h\mathbf{u}\right\|^2+\frac{3N\Delta t\omega}{4}\left\|\frac{8\rho_s\mathcal{P}(q(\hat{C}_h))(1-\omega)}{3\omega}D^{-1/2}\mathbf{u}\right\|^2\\&+\frac{3N\Delta t\omega}{4}\left\|\frac{8}{3}D^{-1/2}\boldsymbol{\nabla}\hat{C}_h\right\|^2+\frac{3N\Delta t\omega}{4}\left\|\frac{8(1-\omega)\rho_s\mathcal{P}^1(q'(\hat{C}_h))}{3\omega}D^{-1/2}\boldsymbol{\nabla}\hat{C}_h\right\|^2\\&+\|\omega C_h^0+(1-\omega)\rho_s q(C_h^0)-2(\omega\hat{C}_h+(1-\omega)\rho_s\mathcal{P}(q(\hat{C}_h)))\|^2.\end{aligned}$$

Theorem 7 *Suppose the assumptions (F1)-(F7) hold, and the fully discrete problem* (13)-(14) *has a solution* $\{C_h^n\}_{n=0}^N\in L^2(0,T;H^1(\Omega))$. *Then we have the following stability result*

$$\begin{aligned}&\|\omega C_h^{N+1}+(1-\omega)\rho_s\mathcal{P}(q(C_h^{N+1}))\|^2+\Delta t\omega\sum_{n=0}^{N}\|\boldsymbol{\nabla}C_h^{n+1/2}\|^2\\&+2\Delta t\omega\sum_{n=0}^{N}\int_{\Gamma_{out}}(C_h^{n+1/2})^2(\mathbf{u}\cdot\overrightarrow{n})ds+4(1-\omega)\Delta t\rho_s\sum_{n=0}^{N}\int_{\Gamma_{out}}Q_h(C_h^{n+1/2})(\mathbf{u}\cdot\overrightarrow{n})ds\\&+4(1-\omega)\Delta t\rho_s\sum_{n=0}^{N}\int_{\Omega}\mathcal{P}^1(q'(C_h^{n+1/2}))(D^{1/2}\boldsymbol{\nabla}C_h^{n+1/2})^2\,d\Omega+\frac{1}{4}\mathcal{E}_h^n\\=&\|\omega C_h^0+(1-\omega)\rho_s\mathcal{P}(q(C_h^0))\|^2+\mathcal{B}_h^n\\&+4\Delta t\sum_{n=0}^{N}(f,\omega C_h^{n+1/2}+(1-\omega)\rho_s\mathcal{P}(q(C_h^{n+1/2}))-(\omega\hat{C}_h+(1-\omega)\rho_s\mathcal{P}(q(\hat{C}_h))))\\&-2N\Delta t\omega\int_{\Gamma_{in}}g_h^2(\mathbf{u}\cdot\overrightarrow{n})ds-4(1-\omega)N\Delta t\rho_s\int_{\Gamma_{in}}Q_h(g_h)(\mathbf{u}\cdot\overrightarrow{n})ds.\end{aligned}$$

Proof Let $\hat{C}_h\in X^h$ such that $\hat{C}_h\big|_{\Gamma_{\text{in}}}=g_h$, and set

$$v_h=\omega C_h^{n+1/2}+(1-\omega)\mathcal{P}(q(C_h^{n+1/2}))-(\omega\hat{C}_h+(1-\omega)\rho_s\mathcal{P}(q(\hat{C}_h)))\in X^h_{0,\Gamma_{\text{in}}}(\Omega).$$

Then, after plugging in v_h, we use the polarization identity to the first term of (13) and (14) and sum the resulting equations to yield

$$\frac{1}{2}(\|\omega C_h^{n+1}+(1-\omega)\rho_s\mathcal{P}(q(C_h^{n+1}))\|^2-\|\omega C_h^n+(1-\omega)\rho_s\mathcal{P}(q(C_h^n))\|^2 \tag{36}$$

$$
\begin{aligned}
&- \|\omega C_h^{n+1/2} + (1-\omega)\rho_s \mathcal{P}((C_h^{n+1/2})) - (\omega C_h^{n+1} + (1-\omega)\rho_s \mathcal{P}(q(C_h^{n+1})))\|^2 \\
&+ \|\omega C_h^{n+1/2} + (1-\omega)\rho_s \mathcal{P}((C_h^{n+1/2})) - (\omega C_h^{n} + (1-\omega)\rho_s \mathcal{P}(q(C_h^{n})))\|^2) \\
&+ \Delta t(\mathbf{u}\cdot \boldsymbol{\nabla} C_h^{n+1/2}, \omega C_h^{n+1/2} + (1-\omega)\mathcal{P}(q(C_h^{n+1/2}))) \\
&+ \Delta t(D\boldsymbol{\nabla} C_h^{n+1/2}, \boldsymbol{\nabla}\Big(\omega C_h^{n+1/2} + (1-\omega)\mathcal{P}(q(C_h^{n+1/2}))\Big)) \\
=\ & \Delta t(f^{n+1/2}, \omega C_h^{n+1/2} + (1-\omega)\mathcal{P}(q(C_h^{n+1/2})) - (\omega \hat{C}_h + (1-\omega)\rho_s \mathcal{P}(q(\hat{C}_h)))) \\
&+ (\omega C_h^{n+1} + (1-\omega)\rho_s q(C_h^{n+1}) - \omega C_h^{n} - (1-\omega)\rho_s q(C_h^{n}), (\omega \hat{C}_h + (1-\omega)\rho_s \mathcal{P}(q(\hat{C}_h))) \\
&+ \Delta t(\mathbf{u}\cdot \boldsymbol{\nabla} C_h^{n+1/2}, \omega \hat{C}_h + (1-\omega)\rho_s \mathcal{P}(q(\hat{C}_h))) + \Delta t(D\boldsymbol{\nabla} C_h^{n+1/2}, \boldsymbol{\nabla}\Big((\omega \hat{C}_h + (1-\omega)\rho_s \mathcal{P}(q(\hat{C}_h)\Big))).
\end{aligned}
$$

Since from (13)-(14) we also have

$$
\begin{aligned}
0 = &- \|\omega C_h^{n+1/2} + (1-\omega)\rho_s \mathcal{P}((C_h^{n+1/2})) - (\omega C_h^{n+1} + (1-\omega)\rho_s \mathcal{P}(q(C_h^{n+1})))\|^2 \\
&+ \|\omega C_h^{n+1/2} + (1-\omega)\rho_s \mathcal{P}((C_h^{n+1/2})) - (\omega C_h^{n} + (1-\omega)\rho_s \mathcal{P}(q(C_h^{n})))\|^2,
\end{aligned}
$$

then

$$
\begin{aligned}
&\frac{1}{2}(\|\omega C_h^{n+1} + (1-\omega)\rho_s \mathcal{P}(q(C_h^{n+1}))\|^2 - \|\omega C_h^{n} + (1-\omega)\rho_s \mathcal{P}(q(C_h^{n}))\|^2) \\
&+ \Delta t(\mathbf{u}\cdot \boldsymbol{\nabla} C_h^{n+1/2}, \omega C_h^{n+1/2} + (1-\omega)\mathcal{P}(q(C_h^{n+1/2}))) \\
&+ \Delta t(D\boldsymbol{\nabla} C_h^{n+1/2}, \boldsymbol{\nabla}\Big(\omega C_h^{n+1/2} + (1-\omega)\mathcal{P}(q(C_h^{n+1/2}))\Big)) \\
=\ & \Delta t(f^{n+1/2}, \omega C_h^{n+1/2} + (1-\omega)\mathcal{P}(q(C_h^{n+1/2})) - (\omega \hat{C}_h + (1-\omega)\rho_s \mathcal{P}(q(\hat{C}_h)))) \\
&+ (\omega C_h^{n+1} + (1-\omega)\rho_s q(C_h^{n+1}) - \omega C_h^{n} - (1-\omega)\rho_s q(C_h^{n}), (\omega \hat{C}_h + (1-\omega)\rho_s \mathcal{P}(q(\hat{C}_h))) \\
&+ \Delta t(\mathbf{u}\cdot \boldsymbol{\nabla} C_h^{n+1/2}, (\omega \hat{C}_h + (1-\omega)\rho_s \mathcal{P}(q(\hat{C}_h))) \\
&+ \Delta t(D\boldsymbol{\nabla} C_h^{n+1/2}, \boldsymbol{\nabla}\Big((\omega \hat{C}_h + (1-\omega)\rho_s \mathcal{P}(q(\hat{C}_h)\Big))).
\end{aligned}
$$

With a technique similar to the one used in the semidiscrete in space case in Theorem 4 we get

$$
\begin{aligned}
&\frac{1}{2}(\|\omega C_h^{n+1} + (1-\omega)\rho_s \mathcal{P}(q(C_h^{n+1}))\|^2 - \|\omega C_h^{n} + (1-\omega)\rho_s \mathcal{P}(q(C_h^{n}))\|^2) + \frac{\omega \Delta t}{4}\|D^{1/2}\boldsymbol{\nabla} C_h^{n+1/2}\|^2 \\
&+ (1-\omega)\Delta t \rho_s \int_{\Gamma_{\text{out}}} Q_h(C_h^{n+1/2})(\mathbf{u}\cdot \overrightarrow{n})ds + \Delta t(1-\omega)\rho_s \int_{\Omega} \mathcal{P}^1(q'(C_h^{n+1/2}))(D^{1/2}\boldsymbol{\nabla} C_h^{n+1/2})^2\, d\Omega \\
&+ \frac{\Delta t\omega}{2}\int_{\Gamma_{\text{out}}} (C_h^{n+1/2})^2(\mathbf{u}\cdot \overrightarrow{n})ds + \frac{3\Delta t\omega}{16}\left\| D^{1/2}\boldsymbol{\nabla} C_h^{n+1/2} - \frac{8}{3}D^{-1/2}\hat{C}_h \mathbf{u}\right\|^2 \\
&+ \frac{3\Delta t\omega}{16}\left\| D^{1/2}\boldsymbol{\nabla} C_h^{n+1/2} - \frac{8\rho_s \mathcal{P}(q(\hat{C}_h))(1-\omega)}{3\omega}D^{-1/2}\mathbf{u}\right\|^2 \\
&+ \frac{3\Delta t\omega}{16}\left\| D^{1/2}\boldsymbol{\nabla} C_h^{n+1/2} - \frac{8}{3}D^{-1/2}\boldsymbol{\nabla}\hat{C}_h\right\|^2 \\
&+ \frac{3\Delta t\omega}{16}\left\| D^{1/2}\boldsymbol{\nabla} C_h^{n+1/2} - \frac{8(1-\omega)\rho_s \mathcal{P}^1(q'(\hat{C}_h))}{3\omega}D^{-1/2}\boldsymbol{\nabla}\hat{C}_h\right\|^2 \\
=\ & \Delta t(f^{n+1/2}, \omega C_h^{n+1/2} + (1-\omega)\rho_s \mathcal{P}(q(C_h^{n+1/2})) - (\omega \hat{C}_h + (1-\omega)\rho_s \mathcal{P}(q(\hat{C}_h)))) \\
&- \frac{\Delta t\omega}{2}\int_{\Gamma_{\text{in}}} g_h^2(\mathbf{u}\cdot \overrightarrow{n})ds + \frac{3\Delta t\omega}{16}\left\|\frac{8}{3}D^{-1/2}\hat{C}_h \mathbf{u}\right\|^2
\end{aligned}
$$

$$+ \frac{3\Delta t\omega}{16}\left\|\frac{8\rho_s\mathcal{P}(q(\hat{C_h}))(1-\omega)}{3\omega}D^{-1/2}\mathbf{u}\right\|^2 + \frac{3\Delta t\omega}{16}\left\|\frac{8}{3}D^{-1/2}\nabla\hat{C_h}\right\|^2$$
$$+ \frac{3\Delta t\omega}{16}\left\|\frac{8(1-\omega)\rho_s\mathcal{P}^1(q'(\hat{C_h}))}{3\omega}D^{-1/2}\nabla\hat{C_h}\right\|^2 - (1-\omega)\rho_s\Delta t\int_{\Gamma_{\text{in}}} Q_h(g_h)(\mathbf{u}\cdot\vec{n})ds$$
$$+ (\omega C_h^{n+1} + (1-\omega)\rho_s q(C_h^{n+1}) - \omega C_h^n - (1-\omega)\rho_s q(C_h^n), (\omega\hat{C_h} + (1-\omega)\rho_s\mathcal{P}(q(\hat{C_h}))).$$

Summation over $n = 0$ to $n = N$ yields the conclusion. □

4.3 Affine Isotherm

In the case of affine adsorption, i.e., $q(C) = K_1 + K_2C$ with $K_1,\ K_2 \geq 0$, we have that $\frac{\partial q}{\partial t} = K_2\frac{\partial C}{\partial t}$, and let us denote $\bar{\omega} = (\omega + (1-\omega)\rho_s K_2)$. The variational formulation (9) then simplifies to: Find $C \in H^1(\Omega)$ such that $C\Big|_{\Gamma_{\text{in}}} = g$ and

$$\left(\bar{\omega}\frac{\partial C}{\partial t}, v\right) + (\mathbf{u}\cdot\nabla C, v) + (D\nabla C, \nabla v) = (f, v), \text{ for all } v \in H^1_{0,\Gamma_{\text{in}}}(\Omega). \tag{37}$$

The semi-discrete in space Finite Element problem (10) with affine adsorption is: Find $C_h \in X^h$ such that $C_h\Big|_{\Gamma_{\text{in}}} = g_h$ and

$$\left(\bar{\omega}\frac{\partial C_h}{\partial t}, v_h\right) + (\mathbf{u}\cdot\nabla C_h, v_h) + (D\nabla C_h, \nabla v_h) = (f, v_h), \text{ for all } v_h \in X^h_{0,\Gamma_{\text{in}}}(\Omega). \tag{38}$$

For the fully discrete analysis, we use the refactorization of midpoint method [65] for time discretization: Given $C_h^n \in X^h$, find $C_h^{n+1} \in X^h$ such that $C_h^{n+1}\Big|_{\Gamma_{\text{in}}} = g_h$ satisfying

Step 1: Backward Euler step at the half-integer time step $t_{n+1/2}$, for all $v_h \in X^h_{0,\Gamma_{\text{in}}}(\Omega)$,

$$\left(\bar{\omega}\frac{C_h^{n+1/2} - C_h^n}{\Delta t/2}, v_h\right) + (u\cdot\nabla C_h^{n+1/2}, v_h) + (D\nabla C_h^{n+1/2}, \nabla v_h) = (f^{n+1/2}, v_h). \tag{39}$$

Step 2: Forward Euler step at t_{n+1}, for all $v_h \in X^h_{0,\Gamma_{\text{in}}}(\Omega)$,

$$\left(\bar{\omega}\frac{C_h^{n+1} - C_h^{n+1/2}}{\Delta t/2}, v_h\right) + (u\cdot\nabla C_h^{n+1/2}, v_h) + (D\nabla C_h^{n+1/2}, \nabla v_h) = (f^{n+1/2}, v_h). \tag{40}$$

The following result gives an *a priori* error estimate for the case of affine adsorption $q(C) = K_1 + K_2C$ and semi-discrete in space approximations.

Theorem 8 *Assume that (F1)-(F6) are satisfied and the variational formulation with affine adsorption given by* (37) *has an exact solution* $C \in H^1(0, T, H^{k+1}(\Omega))$ *and* C_h *solves the* *semi-discrete in space Finite Element formulation with affine adsorption given by* (38). *Then for* $1 \le r \le k+1$ *there exists a positive constant* K *independent of* h *such that:*

$$\|C - C_h\|_{L^2(0,T;H^1(\Omega))} \le \left(h^{r-1}\|C\|_{L^2(0,T;H^r(\Omega))} + h^{r-1}\left\|\frac{\partial C}{\partial t}\right\|_{L^2(0,T;H^r(\Omega))} + \|(C_h - \hat{C}_h)(0)\| \right) \times \left(\max\left\{ \left(2 + \frac{8K_{PF}^2\|\mathbf{u}\|_\infty^2 + 8\beta_1^2}{\lambda^2}\right) K_1^2, \frac{8K_{PF}^2\omega^2}{\lambda^2}K_1^2, \frac{4\omega}{\lambda} \right\} \right)^{1/2}.$$

Remark 6 *The argument is the same as in the nonlinear case, see Theorem 5.*

Next, we prove an energy type bound for (39)-(40), the discrete version of the adsorption equation (1) for the affine isotherm, using the midpoint method for the time discretization.

Theorem 9 *Suppose the assumptions (F1)-(F7) hold, and the fully discrete problem* (39)-(40) *has a smooth solution* $\{C_h^n\}_{n=0}^N \in L^2(0,T;H^1(\Omega))$. *Then*

$$\|C_h^N\|^2 + \frac{2}{\bar{\omega}}\Delta t \sum_{n=0}^{N-1} \left(\int_{\Gamma_{out}} ((C_h^{n+1/2})^2)(\mathbf{u}\cdot\vec{n})ds \right) + \frac{\lambda}{\bar{\omega}}\Delta t \sum_{n=0}^{N-1} \|\nabla C_h^{n+1/2}\|^2$$
$$\le \frac{4N\Delta t\|\mathbf{u}\|_\infty^2 + 8\lambda\omega}{\bar{\omega}\lambda}\|\hat{C}_h\|^2 + \frac{2N\Delta t}{\bar{\omega}}\left(\int_{\Gamma_{in}} ((g_h)^2)(-\mathbf{u}\cdot\vec{n})ds \right) + \frac{4N\Delta t\beta_1^2 + N\Delta t\lambda^2}{\bar{\omega}\lambda}\|\nabla\hat{C}_h\|^2$$
$$+ \frac{8K_{PF}^2}{\bar{\omega}\lambda}\Delta t \sum_{n=0}^{N-1} \|f^{n+1/2}\|^2 + 3\|C_h^0\|^2.$$

Proof Let $\hat{C}_h \in X^h$ be such that $\hat{C}_h\big|_{\Gamma_{in}} = g_h$ and take $v_h = C_h^{n+1/2} - \hat{C}_h \in X_{0,\Gamma_{in}}^h(\Omega)$. After plugging in v_h, we use the polarization identity to the first term of (39) and (40) and sum the resulting equations to yield

$$\frac{\bar{\omega}}{2}(\|C_h^{n+1}\|^2 - \|C_h^n\|^2) + \Delta t(\mathbf{u}\cdot\nabla C_h^{n+1/2}, C_h^{n+1/2}) + \Delta t(D\nabla C_h^{n+1/2}, \nabla C_h^{n+1/2})$$
$$= \Delta t(f^{n+1/2}, C_h^{n+1/2} - \hat{C}_h) + (\bar{\omega}(C_h^{n+1} - C_h^n), \hat{C}_h) + \Delta t(\mathbf{u}\cdot\nabla C_h^{n+1/2}, \hat{C}_h) + \Delta t(D\nabla C_h^{n+1/2}, \nabla\hat{C}_h).$$

Using

$$(\mathbf{u}\cdot\nabla C_h^{n+1/2}, C_h^{n+1/2}) = \frac{1}{2}\left(\int_{\Gamma_{in}} ((g_h)^2)(\mathbf{u}\cdot\vec{n})ds \right) + \frac{1}{2}\left(\int_{\Gamma_{out}} ((C_h^{n+1/2})^2)(\mathbf{u}\cdot\vec{n})ds \right),$$

and standard estimates we further obtain

$$\frac{\bar{\omega}}{2}\|C_h^{n+1}\|^2 - \frac{\bar{\omega}}{2}\|C_h^n\|^2 + \frac{\Delta t}{2}\left(\int_{\Gamma_{out}} ((C_h^{n+1/2})^2)(\mathbf{u}\cdot\vec{n})ds \right) + \frac{\Delta t\lambda}{4}\|\nabla C_h^{n+1/2}\|^2$$
$$\le \frac{\|\mathbf{u}\|_\infty^2\Delta t}{\lambda}\|\hat{C}_h\|^2 - \frac{\Delta t}{2}\left(\int_{\Gamma_{in}} ((g_h)^2)(\mathbf{u}\cdot\vec{n})ds \right) + \frac{\Delta t\beta_1^2}{\lambda}\|\nabla\hat{C}_h\|^2$$
$$+ \frac{2K_{\text{PF}}^2\Delta t}{\lambda}\|f^{n+1/2}\|^2 + \frac{\Delta t\lambda}{4}\|\nabla\hat{C}_h\|^2 + (\bar{\omega}(C_h^{n+1} - C_h^n), \hat{C}_h),,$$

which by summation over $n = 0$ to $n = N-1$ concludes the argument. □

Remark 7 *We note that an intermediate result in the previous proof gives*

$$\frac{\bar{\omega}}{2}\|C_h^{n+1}\|^2 - \frac{\bar{\omega}}{2}\|C_h^n\|^2 + \frac{\Delta t}{2}\left(\int_{\Gamma_{out}}((C_h^{n+1/2})^2)(\mathbf{u}\cdot\overrightarrow{n})ds\right) + \Delta t(D\boldsymbol{\nabla} C_h^{n+1/2}, \boldsymbol{\nabla} C_h^{n+1/2})$$
$$= -\frac{\Delta t}{2}\left(\int_{\Gamma_{in}}((g_h)^2)(\mathbf{u}\cdot\overrightarrow{n})ds\right) + \Delta t(f^{n+1/2}, C_h^{n+1/2} - \hat{C}_h)$$
$$+ (\bar{\omega}(C_h^{n+1} - C_h^n), \hat{C}_h) + \Delta t(\mathbf{u}\cdot\boldsymbol{\nabla} C_h^{n+1/2}, \hat{C}_h) + \Delta t(D\boldsymbol{\nabla} C_h^{n+1/2}, \boldsymbol{\nabla}\hat{C}_h),$$

which when $f = 0$ and $\hat{C}_h = 0$ yields the following the mass balance type relation

$$\frac{\bar{\omega}}{2}(\|C_h^{n+1}\|^2 - \|C_h^n\|^2) + \frac{\Delta t}{2}\left(\int_{\Gamma_{out}}((C_h^{n+1/2})^2)(\mathbf{u}\cdot\overrightarrow{n})ds\right) + \Delta t(D\boldsymbol{\nabla} C_h^{n+1/2}, \boldsymbol{\nabla} C_h^{n+1/2})$$
$$= \frac{\Delta t}{2}\left(\int_{\Gamma_{in}}((g_h)^2)(-\mathbf{u}\cdot\overrightarrow{n})ds\right),$$

where $\mathbf{u}\cdot\overrightarrow{n} < 0$ on Γ_{in}.

Finally, we provide an *a priori* error estimate for the case of affine adsorption in the fully discrete case (39)-(40).

Theorem 10 *Suppose the assumptions (F1)-(F7) are satisfied,* (39)-(40) *has a solution $\{C_h^n\}_{n=0}^N \in L^2(0,T;H^1(\Omega))$, and* (37) *has an exact solution $C \in H^1(0,T,H^{k+1}(\Omega))$. Then for all $1 \le r \le k+1$:*

$$\Delta t\sum_{n=0}^N \|C(t_{n+1/2}) - C_h(t_{n+1/2})\|_1^2 \le \max\left\{\left(2 + \frac{8K_{PF}^2\|\mathbf{u}\|_\infty^2 + 8\beta_1^2}{\lambda^2}\right)K_2^2, \frac{8K_{PF}^2\bar{\omega}^2}{\lambda^2}K_2^2, \frac{TK_{PF}^2}{3\lambda^2}, \frac{2\bar{\omega}}{\lambda}\right\}$$
$$\times\left(h^{2r-2}\Delta t\sum_{n=0}^N \|C(t_{n+1/2})\|_r^2 + h^{2r-2}\left\|\frac{\partial C}{\partial t}\right\|_{L^2(0,T;H^r(\Omega))}^2 + (\Delta t)^4\|C_{ttt}\|_{L^\infty(0,T;L^\infty)}^2 + \|\hat{C}_h - C_h^0\|^2\right).$$

Proof Let the approximate solution at time $t^{n+1/2}$ be $C_h^{n+1/2}$. Then by using the midpoint method, we get, the fully discrete variational formulation as follows:
Given $C_h^n \in X^h$, find $C_h^{n+1} \in X^h$ such that $C_h^{n+1}\Big|_{\Gamma_{\text{in}}} = g_h$ and satisfying,

$$\left(\bar{\omega}\frac{C_h^{n+1} - C_h^n}{\Delta t}, v_h\right) + (u\cdot\boldsymbol{\nabla} C_h^{n+1/2}, v_h) + (D\boldsymbol{\nabla} C_h^{n+1/2}, \boldsymbol{\nabla} v_h) = (f^{n+1/2}, v_h),\ \forall v_h \in X_{0,\Gamma_{\text{in}}}^h(\Omega). \tag{41}$$

Let C_t represent $\frac{\partial C}{\partial t}$. We write the following variational formulation for the exact solution $C(t)$.

$$\left(\bar{\omega}\frac{C(t_{n+1}) - C(t_n)}{\Delta t}, v\right) + (\mathbf{u}\cdot\boldsymbol{\nabla} C(t_{n+1/2}), v) + (D\boldsymbol{\nabla} C(t_{n+1/2}), \boldsymbol{\nabla} v)$$
$$= (f^{n+1/2}, v) + (r^n, v),\ \forall\ v \in H_{0,\Gamma_{\text{in}}}^1(\Omega). \tag{42}$$

where time discretization error, $r^n = \frac{C(t_{n+1}) - C(t_n)}{\Delta t} - \frac{C_t(t_{n+1}) + C_t(t_n)}{2}$.
Let $e^n = C(t_n) - C_h^n$ and $v = v_h \in X_{0,\Gamma_{\text{in}}}^h \subset H_{0,\Gamma_{\text{in}}}^1(\Omega)$ in (42) and then subtract (41) from (42) to get

$$\left(\bar{\omega}\frac{e^{n+1} - e^n}{\Delta t}, v_h\right) + (\mathbf{u}\cdot\boldsymbol{\nabla} e^{n+1/2}, v_h) + (D\boldsymbol{\nabla} e^{n+1/2}, \boldsymbol{\nabla} v_h) = (r^n, v_h),\quad \forall v_h \in X_{0,\Gamma_{\text{in}}}^h(\Omega).$$

Consider $\hat{C}_h \in X^h$ such that $\hat{C}_h\Big|_{\Gamma_{\text{in}}} = g_h$. Then $e^n = C(t_n) - C_h^n = \phi_h^n + \eta^n$, where $\phi_h^n = \hat{C}_h - C_h^n$ and $\eta^n = \hat{C}_h - C(t_n)$. Choosing $v_h = \phi_h^{n+1/2} \in X^h_{0,\Gamma_{\text{in}}}$, the above error equation becomes

$$\Big(\bar{\omega}\frac{\phi_h^{n+1} - \phi_h^n}{\Delta t}, \phi_h^{n+1/2}\Big) + (\mathbf{u}\cdot\boldsymbol{\nabla}\phi_h^{n+1/2}, \phi_h^{n+1/2}) + (D\boldsymbol{\nabla}\phi_h^{n+1/2}, \boldsymbol{\nabla}\phi_h^{n+1/2})$$
$$= \Big(\bar{\omega}\frac{\eta^{n+1} - \eta^n}{\Delta t}, \phi_h^{n+1/2}\Big) + (\mathbf{u}\cdot\boldsymbol{\nabla}\eta^{n+1/2}, \phi_h^{n+1/2}) + (D\boldsymbol{\nabla}\eta^{n+1/2}, \boldsymbol{\nabla}\phi_h^{n+1/2}) + (r^n, \phi_h^{n+1/2}).$$

With a technique similar to one used in Theorem 8 and a Taylor expansion for the residual r^n we obtain

$$\|\phi_h^N\|^2 + \frac{\lambda}{\bar{\omega}}\sum_{n=0}^{N}\Delta t\|\boldsymbol{\nabla}\phi_h^{n+1/2}\|^2 \leq \Big(\frac{4K_{\text{PF}}^2\|\mathbf{u}\|_\infty^2 + 4\beta_1^2}{\bar{\omega}\lambda}\Big)\sum_{n=0}^{N}\Delta t\|\eta^{n+1/2}\|_1^2 + \frac{4K_{\text{PF}}^2\bar{\omega}}{\lambda}\int_0^T \|\eta_t\|^2 dt$$
$$+ \frac{TK_{\text{PF}}^2}{6\bar{\omega}\lambda}(\Delta t^2\|C_{ttt}\|_{L^\infty(0,T;L^\infty)})^2 + \|\phi_h^0\|^2.$$

Since by the triangle inequality we have

$$\sum_{n=0}^{N}\Delta t\|e^{n+1/2}\|_1^2 \leq \sum_{n=0}^{N}2\Delta t\Big(\|\phi_h^{n+1/2}\|_1^2 + \|\eta^{n+1/2}\|_1^2\Big),$$

the errors satisfy

$$\sum_{n=0}^{N}\Delta t\|e^{n+1/2}\|_1^2 \leq \Big(2 + \frac{8K_{\text{PF}}^2\|\mathbf{u}\|_\infty^2 + 8\beta_1^2}{\lambda^2}\Big)\Delta t\sum_{n=0}^{N}\inf_{\substack{\hat{C_h}\in X^h\\ \hat{C_h}|_{\Gamma_{\text{in}}}=g_h}}\|C^{n+1/2} - \hat{C}_h\|_1^2$$
$$+ \frac{8K_{\text{PF}}^2\bar{\omega}^2}{\lambda^2}\int_0^T \inf_{\substack{\hat{C_h}\in X^h\\ \hat{C_h}|_{\Gamma_{\text{in}}}=g_h}}\Big\|\frac{\partial(C - \hat{C}_h)}{\partial t}\Big\|^2 dt + \frac{TK_{\text{PF}}^2}{3\lambda^2}(\Delta t^2\|C_{ttt}\|_{L^\infty(0,T;L^\infty)})^2 + \frac{2\bar{\omega}}{\lambda}\|\phi_h^0\|^2.$$

Choosing g_h the interpolant of g in $X^h_{\Gamma_{\text{in}}}$, Lemma 3 concludes the argument. □

5 Numerical Test

In this section, we perform numerical tests to show that the midpoint method described in Section 3.2 gives a second-order convergence rate for the considered PDE model for the constant, affine, and nonlinear, explicit adsorptions. Since the results are similar, we only show the nonlinear, explicit adsorption case. In the following two subsections, we first check the convergence rate for the case of nonlinear, explicit isotherm in the first test, and in the second test, we plot the concentration profile. We also show the comparison of total mass after each test. In order to reduce the computational cost, for the numerical results in this section we use a 2D spatial domain $\Omega = [0,1]^2 \subset \mathbb{R}^2$, representing a cross-section through the center of the cylinder in Figure 1. The numerical parameters are chosen to be representative of commonly used test cases [9] in the numerical analysis literature and are intended to illustrate the theoretical properties of the scheme.

5.1 Convergence Results

For checking the order of convergence, we assume the following: $\mathbf{u} = (1,1)$, $D = I$, $\Omega = [0,1] \times [0,1]$, $\omega = 0.5$, $X^h =$ the space of continuous piecewise affine functions, the exact solution is $C(x,y,t) = t^2(x^3 - \frac{3}{2}x^2 + 1)\cos(\frac{\pi}{4}y)$. The true solution determines the body force f, initial condition C_0, and boundary conditions. The norms used in the table are defined as follows,

$$\|C\|_{\infty,0} := \text{ess} \sup_{0<t<T} \|C(\cdot,t)\|_{L^2(\Omega)} \text{ and } \|C\|_{0,0} := \left(\int_0^T \|C(\cdot,t)\|^2_{L^2(\Omega)}\, dt \right)^{1/2}.$$

In this test problem, we use Langmuir's isotherm with $q_{max} = K_{eq} = 1$ where $q(C) = \frac{q_{max} K_{eq} C}{1+K_{eq}C} = \frac{C}{1+C}$. We simplify the problem formulation to a single (nonlinear) transport equation in one unknown C using

$$\frac{\partial q}{\partial t} = \frac{\partial q}{\partial C}\frac{\partial C}{\partial t} = \frac{1}{(1+C)^2}\frac{\partial C}{\partial t}.$$

While using Backward Euler discretization, we compute solutions by lagging the nonlinearity $q'(C_h^{n+1})$ as [80]

$$q'(C_h^{n+1})\frac{C_h^{n+1} - C_h^n}{\Delta t} \approx q'(C_h^n)\frac{C_h^{n+1} - C_h^n}{\Delta t}.$$

For the midpoint method, we use the standard (second order) linear extrapolation[81] of $C_h^{n+1/2}$ while computing $q'(C_h^{n+1/2})$ as

$$q'(C_h^{n+1/2})\frac{C_h^{n+1} - C_h^n}{\Delta t} \approx q'\left(\frac{3C_h^n - C_h^{n-1}}{2}\right)\frac{C_h^{n+1} - C_h^n}{\Delta t}.$$

Table 1 reports BE temporal errors at fixed $h = 1/128$ and the experimental order of convergence is 1, which matches the first order precision of the scheme.

$(h, \Delta t)$ $\rightarrow$	$(1/128, 1/2)$	$(1/128, 1/4)$	$(1/128, 1/8)$	$(1/128, 1/16)$	$(1/128, 1/32)$
$\|C - C_h\|_{\infty,0}$	0.0636074	0.0374917	0.0206665	0.0108985	0.00558454
Rate	-	0.76262	0.85928	0.92316	0.96462
$\|C - C_h\|_{0,0}$	0.0522838	0.0310798	0.0169125	0.00883222	0.00451535
Rate	-	0.75039	0.87789	0.93724	0.96794
$\|\nabla C - \nabla C_h\|_{0,0}$	0.0847469	0.0502647	0.0273473	0.0143409	0.00746467
Rate	-	0.75362	0.87815	0.93126	0.94199
$\|C - C_h\|_{0,1}$	0.0995773	0.0590973	0.0321544	0.0168424	0.00872408
Rate	-	0.75272	0.87808	0.93292	0.94902

Table 1: Temporal convergence rates for the BE approximation with a Langmuir adsorption model to the non-steady-state problem.

Table 2 shows midpoint temporal errors whose experimental order is 2 in all norms, consistent with the scheme's second-order accuracy in the fully discrete analysis Theorem 10. Figure 2 compares BE and midpoint at $h = 1/128$, the lines have

$(h, \Delta t)$ $\rightarrow$	$(1/128, 1/2)$	$(1/128, 1/4)$	$(1/128, 1/8)$	$(1/128, 1/16)$	$(1/128, 1/32)$
$\|C - C_h\|_{\infty,0}$	0.0357416	0.00951864	0.00242801	0.000611192	0.000153313
Rate	-	1.9088	1.971	1.9901	1.9951
$\|C - C_h\|_{0,0}$	0.0307399	0.00741601	0.00181065	0.00044712	0.000111214
Rate	-	2.0514	2.0341	2.0178	2.0073
$\|\nabla C - \nabla C_h\|_{0,0}$	0.744766	0.191186	0.0475431	0.0117471	0.00323681
Rate	-	1.9618	2.0077	2.0169	1.8597
$\|C - C_h\|_{0,1}$	0.7454	0.19133	0.0475776	0.0117556	0.00323872
Rate	-	1.962	2.0077	2.0169	1.8599

Table 2: Temporal convergence rates for the midpoint approximation with a Langmuir adsorption model to the non-steady-state problem.

log–log slopes 1 and 2, respectively, as predicted by our analysis.

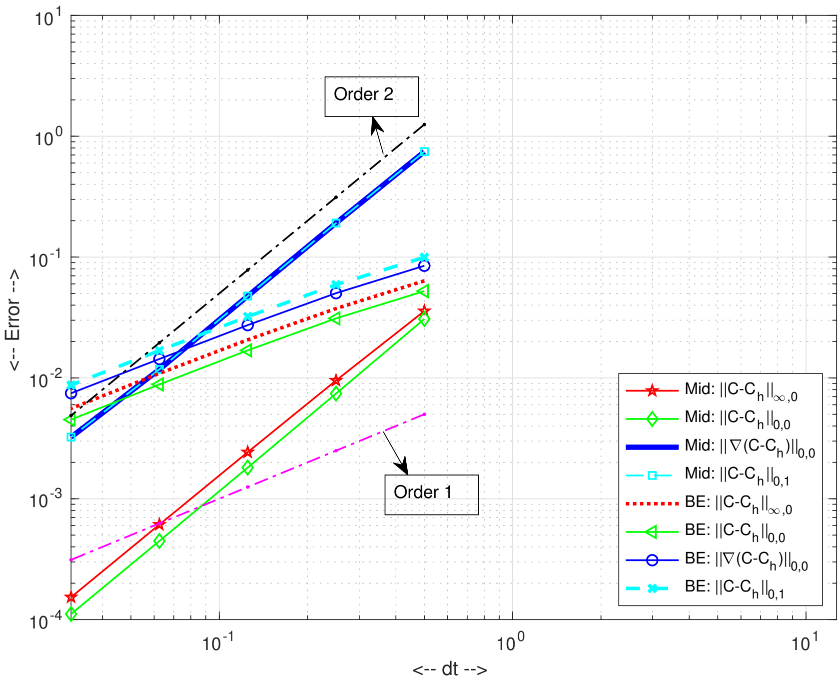

Fig. 2: Langmuir Isotherm: Temporal rate of convergence of BE and Midpoint, $T = 1.0$, $h = 1/128$. Notice that Midpoint is giving order 2 whereas BE is giving order 1.

Figure 3 plots total-mass versus time. The midpoint method nearly preserves mass, whereas BE shows an upward deviation, which agrees with our mass-balance relation in Theorem 2 and the discrete stability bound for the midpoint scheme in Theorem 7.

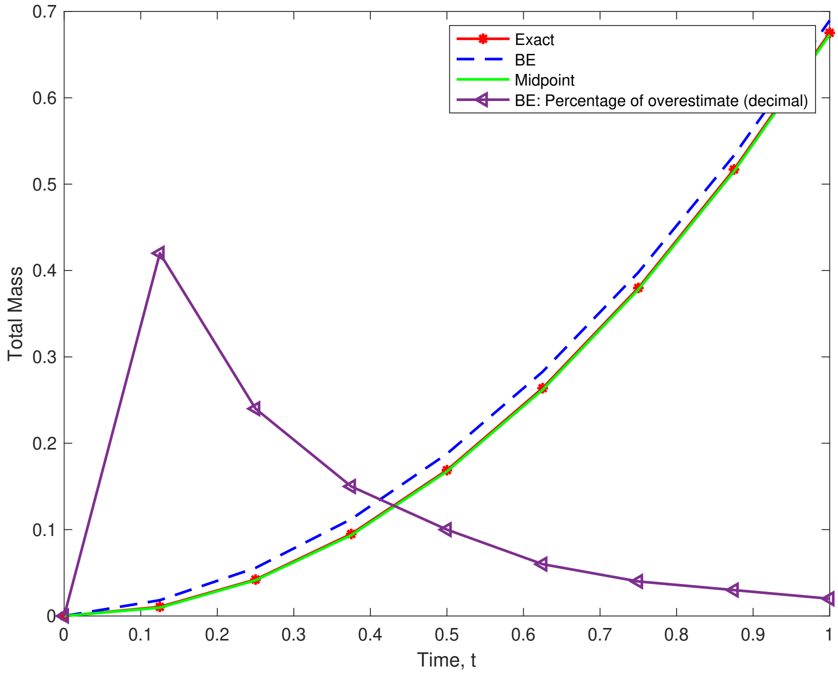

Fig. 3: Langmuir Isotherm: Comparison of total mass for exact solution, BE, Midpoint, $T = 1.0$, $h = 1/128$, $dt = 1/8$. Notice that BE overestimates total mass rather than underestimates.

5.2 Concentration Profiles

For the plot of the concentration profile in each case, we consider the following: $f = 0$, $g = 1$, $T = 0.1$ and $T = 3.0$, $h = 1/128$, $dt = 1/128$, $\mathbf{u} = (0, 2x(x-2))$, $D = I$, $\Omega = [0, 2] \times [0, 10]$, $\omega = 0.5$, $X^h =$ the space of continuous piecewise affine functions.

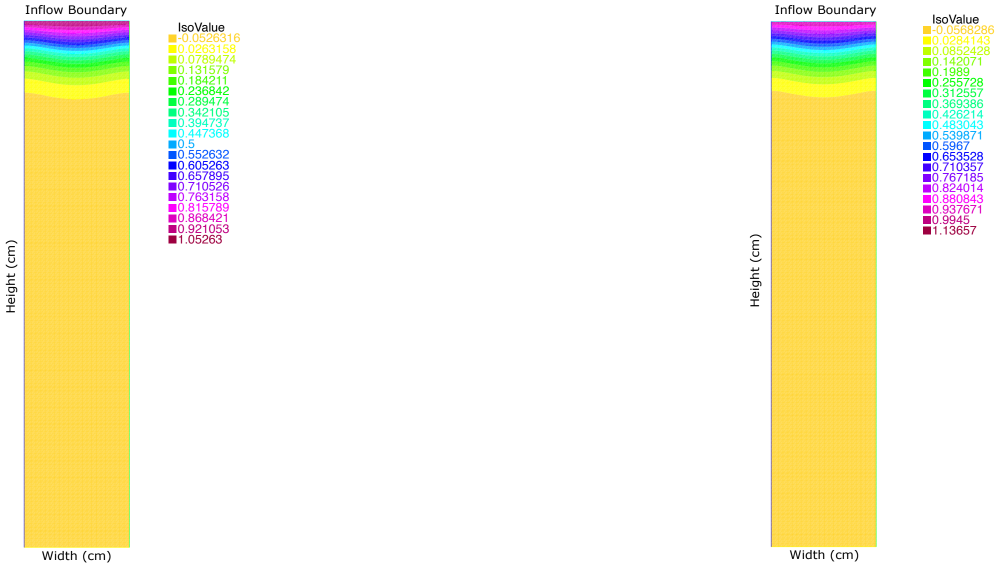

Fig. 4: Langmuir isotherm: The evolution of the concentration in the membrane while using BE (Left) & Midpoint (Right), $\Omega = [0,2] \times [0,10]$, $f = 0$, $g = 1$, $T = 0.1$, $h = 1/128$, $dt = 1/128$, $\mathbf{u} = (0, 2x(x-2))$, $D = I$.

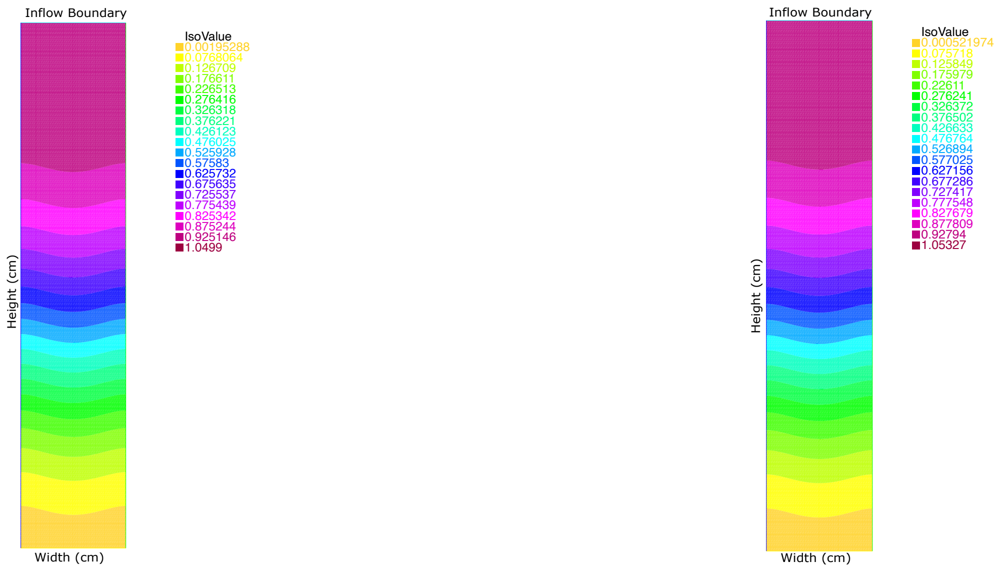

Fig. 5: Langmuir isotherm: The evolution of the concentration in the membrane while using BE (Left) & Midpoint (Right), $\Omega = [0,2] \times [0,10]$, $f = 0$, $g = 1$, $T = 3.0$, $h = 1/128$, $dt = 1/128$, $\mathbf{u} = (0, 2x(x-2))$, $D = I$.

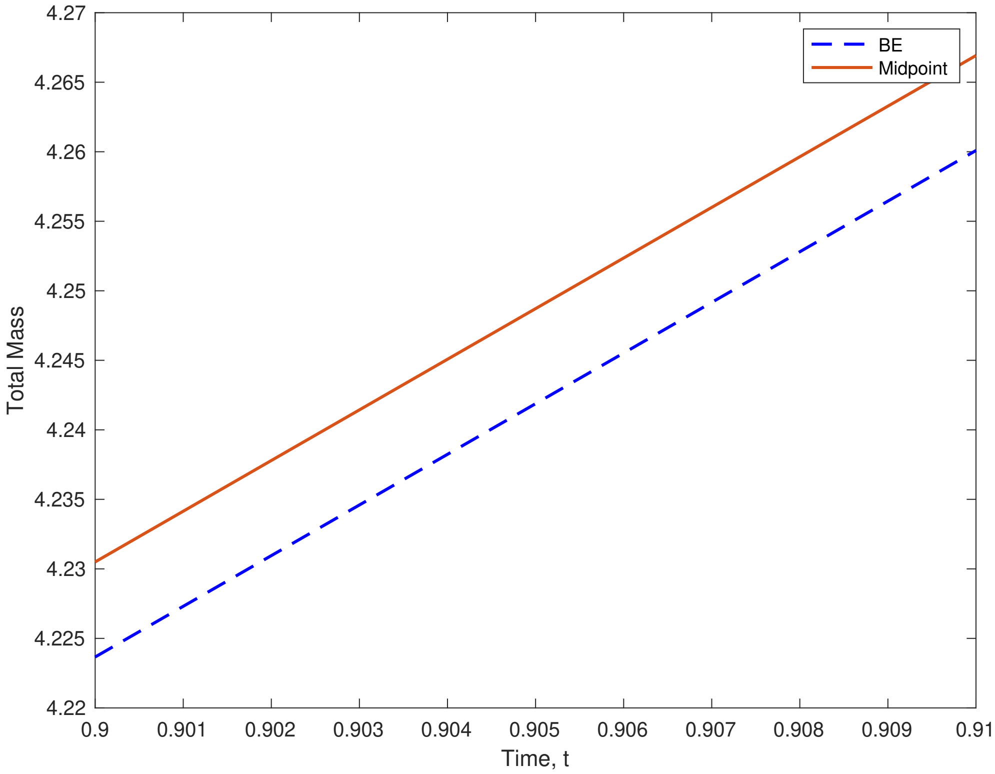

Fig. 6: Langmuir isotherm: Comparison of total mass, $\Omega = [0,2] \times [0,10]$, $f = 0$, $g = 1$, $T = 3.0$, $h = 1/128$, $dt = 1/128$, $\mathbf{u} = (0, 2x(x-2))$, $D = I$.

In Figures 4 and 5, the concentration front gradually advances through the height of the membrane (top to bottom) over time as it evolves following the contour of the velocity profile. Although we cannot visibly see the difference between two plots for BE and midpoint in Figure 5, we can see the significant difference in total mass evolution in Figure 6.

6 Conclusion

We provided a detailed stability and error analysis of a simulation tool for modeling the adsorption process for the constant and affine adsorption cases. For the nonlinear, explicit adsorption, we proved stability analysis for the continuous case and semi-discrete case and the existence of a solution for the fully discrete case. The error analysis for this case is more involved and under some assumptions, we were able to show an error estimate for the semi-discrete case. But numerically, we showed that the midpoint method gives second-order convergence for all adsorption cases. The next most important step in developing this tool is coupling this reactive transport problem with porous media flow where velocity is approximated.

Acknowledgements. We thank Professor William J. Layton, for his insightful idea and guidance throughout the research.

Declarations

- Funding: Farjana Siddiqua is partially supported by the National Science Foundation under grant DMS-2110379. Catalin Trenchea is partially supported by the National Science Foundation under grant 2208220.
- Conflict of interest: The authors declare no competing interests.
- Ethics approval and consent to participate: Not Applicable.
- Consent for publication: All authors approve the submission.
- Data availability: Data sharing is not applicable to this article as no data sets were generated or analyzed during the current study.
- Materials availability: Upon request.
- Code availability: Upon request.
- Author contribution:
  - Conceptualization: Farjana Siddiqua, Catalin Trenchea.
  - Analysis: Farjana Siddiqua.
  - Coding: Farjana Siddiqua.
  - Writing – Original Draft: Farjana Siddiqua
  - Writing – Review & Editing: Farjana Siddiqua, Catalin Trenchea.

References

[1] Biopharmaceutical Market Size to Hit US $856.1 Billion by 2030. https://www.globenewswire.com/news-release/2021/12/22/2357003/0/en/Biopharmaceutical-Market-Size-to-Hit-US-856-1-Bn-by-2030.html. Precedence Research, Accessed: 2022-08-01

[2] Coker, V.: Biotherapeutics outpace conventional therapies. BioPharm International **25**(3), 20–23 (2012)

[3] Leader, B., Baca, Q.J., Golan, D.E.: Protein therapeutics: a summary and pharmacological classification. Nature Reviews Drug Discovery **7**(1), 21–39 (2008)

[4] Quinteros, D.A., Bermúdez, J.M., Ravetti, S., Cid, A., Allemandi, D.A., Palma, S.D.: Therapeutic use of monoclonal antibodies: general aspects and challenges for drug delivery, 807–833 (2017)

[5] Anti-SARS-CoV-2 Monoclonal Antibodies. https://www.covid19treatmentguidelines.nih.gov/therapies/anti-sars-cov-2-antibody-products/anti-sars-cov-2-monoclonal-antibodies/. Accessed: 2022-08-18

[6] COVID-19 Treatments and Medications. https://www.cdc.gov/coronavirus/

2019-ncov/your-health/treatments-for-severe-illness.html. Accessed: 2022-10-19

[7] Coronavirus (COVID-19) Update: FDA Authorizes New Monoclonal Antibody for Treatment of COVID-19 that Retains Activity Against Omicron Variant. https://www.fda.gov/news-events/press-announcements/. Accessed: 2022-02-11

[8] Clarke, K.G.: Bioprocess engineering: an introductory engineering and life science approach (2013)

[9] Wilson, A.B.: Modeling, analysis, and simulation of adsorption in functionalized membranes. PhD thesis, Clemson University (2016)

[10] Wang, J.: Development of a new multimodal membrane adsorber and its application in Chromatographic Bioseparations. PhD thesis, Clemson University (2016)

[11] Bhattacharjee, S., Dong, J., Ma, Y., Hovde, S., Geiger, J.H., Baker, G.L., Bruening, M.L.: Formation of high-capacity protein-adsorbing membranes through simple adsorption of poly (acrylic acid)-containing films at low ph. Langmuir **28**(17), 6885–6892 (2012)

[12] Bhut, B.V., Husson, S.M.: Dramatic performance improvement of weak anion-exchange membranes for chromatographic bioseparations. Journal of Membrane Science **337**(1-2), 215–223 (2009)

[13] Bhut, B.V., Wickramasinghe, S.R., Husson, S.M.: Preparation of high-capacity, weak anion-exchange membranes for protein separations using surface-initiated atom transfer radical polymerization. Journal of Membrane Science **325**(1), 176–183 (2008)

[14] Carta, G., Jungbauer, A.: Protein Chromatography: Process Development and Scale-up. John Wiley & Sons, (2020)

[15] Ghosh, R.: Principles of Bioseparations Engineering. World Scientific Publishing company, (2006)

[16] Yamamoto, S., Nakanishi, K., Matsuno, R.: Ion-exchange Chromatography of Proteins. CRC press, (1988)

[17] Tennikova, T., Freitag, R.: High-performance Membrane Chromatography of Proteins, pp. 255–300. CRC Press, (2020)

[18] Boi, C., Malavasi, A., Carbonell, R.G., Gilleskie, G.: A direct comparison between membrane adsorber and packed column chromatography performance. Journal of Chromatography A **1612**, 460629 (2020)

[19] Shukla, A.A., Hubbard, B., Tressel, T., Guhan, S., Low, D.: Downstream processing of monoclonal antibodies—application of platform approaches. Journal of

Chromatography B **848**(1), 28–39 (2007)

[20] Pollard, D.J., Woodley, J.M.: Biocatalysis for pharmaceutical intermediates: the future is now. TRENDS in Biotechnology **25**(2), 66–73 (2007)

[21] Lott, P.A., Walker, H.F., Woodward, C.S., Yang, U.M.: An accelerated Picard method for nonlinear systems related to variably saturated flow. Advances in Water Resources **38**, 92–101 (2012)

[22] Schneid, E., Knabner, P., Radu, F.: A priori error estimates for a mixed finite element discretization of the Richards' equation. Numerische Mathematik **98**(2), 353–370 (2004)

[23] Radu, F., Pop, I.S., Knabner, P.: Order of convergence estimates for an Euler implicit, mixed finite element discretization of Richards' equation. SIAM J. Numer. Anal. **42**(4), 1452–1478 (2004) https://doi.org/10.1137/S0036142902405229

[24] List, F., Radu, F.A.: A study on iterative methods for solving Richards' equation. Comput. Geosci. **20**(2), 341–353 (2016) https://doi.org/10.1007/s10596-016-9566-3

[25] Radu, F.A., Pop, I.S.: Newton method for reactive solute transport with equilibrium sorption in porous media. J. Comput. Appl. Math. **234**(7), 2118–2127 (2010) https://doi.org/10.1016/j.cam.2009.08.070

[26] Radu, F.A., Pop, I.S., Attinger, S., Knabner, P.: Error estimates for an euler implicit-mixed finite element scheme for reactive transport in saturated/unsaturated soil. PAMM **7**(1), 1024705–1024706 (2007) https://doi.org/10.1002/pamm.200700428 https://onlinelibrary.wiley.com/doi/pdf/10.1002/pamm.200700428

[27] Correa, M.R., Murad, M.A.: Fixed-stress sequential schemes for a black-oil model in poroelastic media. J. Comput. Phys. **543**, 114406–39 (2025) https://doi.org/10.1016/j.jcp.2025.114406

[28] Murad, M.A., Borges, M., Obregón, J.A., Correa, M.R.: A new locally conservative numerical method for two-phase flow in heterogeneous poroelastic media. Computers and Geotechnics **48**, 192–207 (2013)

[29] Jones, G.S., Trenchea, C.: Discrete energy balance equation via a symplectic second-order method for two-phase flow in porous media. Appl. Math. Comput. **480**, 128909 (2024) https://doi.org/10.1016/j.amc.2024.128909

[30] De Marsily, G.: Quantitative hydrogeology: Groundwater hydrology for engineers academic press. Inc., Orlando, Florida (1986)

[31] Bear, J.: Dynamics of fluids in porous media (1988)

[32] Singh, N., Wang, J., Ulbricht, M., Wickramasinghe, S.R., Husson, S.M.: Surface-initiated atom transfer radical polymerization: A new method for preparation of polymeric membrane adsorbers. Journal of Membrane Science **309**(1-2), 64–72 (2008)

[33] Bank, R.E., Bürgler, J.F., Fichtner, W., Smith, R.K.: Some upwinding techniques for finite element approximations of convection-diffusion equations. Numerische Mathematik **58**(1), 185–202 (1990)

[34] Bouloutas, E.T., Celia, M.A.: An improved cubic Petrov-Galerkin method for simulation of transient advection-diffusion processes in rectangularly decomposable domains. Computer Methods in Applied Mechanics and Engineering **92**(3), 289–308 (1991)

[35] Codina, R.: Comparison of some finite element methods for solving the diffusion-convection-reaction equation. Computer Methods in Applied Mechanics and Engineering **156**(1-4), 185–210 (1998)

[36] Heinrichs, W.: Defect correction for convection-dominated flow. SIAM Journal on Scientific Computing **17**(5), 1082–1091 (1996)

[37] Houston, P., Schwab, C., Süli, E.: Stabilized hp-finite element methods for first-order hyperbolic problems. SIAM Journal on Numerical Analysis **37**(5), 1618–1643 (2000)

[38] Johnson, C.: Numerical solution of partial differential equations by the finite element method (2012)

[39] Wilson, A.B., Jenkins, E.W.: Analysis of a fully implicit SUPG scheme for a filtration and separation model. Computational and Applied Mathematics **39**(2), 1–19 (2020)

[40] Wilson, A.B., Jenkins, E.W., Wang, J., Husson, S.M.: Numerical simulation of chemical separations using multimodal adsorption isotherms. Results in Applied Mathematics **7**, 100122 (2020)

[41] Wang, J., Jenkins, E.W., Robinson, J.R., Wilson, A., Husson, S.M.: A new multimodal membrane adsorber for monoclonal antibody purifications. Journal of membrane science **492**, 137–146 (2015)

[42] Wang, J., Zhou, J., Gowtham, Y.K., Harcum, S.W., Husson, S.M.: Antibody purification from CHO cell supernatant using new multimodal membranes. Biotechnology Progress **33**(3), 658–665 (2017)

[43] List, F., Radu, F.A.: A study on iterative methods for solving Richards' equation. Computational Geosciences **20**(2), 341–353 (2016)

[44] Mitra, K., Vohralík, M.: A posteriori error estimates for the Richards equation. Mathematics of Computation **93**(347), 1053–1096 (2024)

[45] Congreve, S., Dolejší, V., Sakić, S.: Error analysis for local discontinuous Galerkin semidiscretization of Richards' equation. IMA Journal of Numerical Analysis **45**(1), 580–630 (2025)

[46] Difonzo, F.V., Pellegrino, S.F.: Convergence analysis of a spectral numerical method for a peridynamic formulation of Richards' equation. Mathematics and Computers in Simulation **223**, 219–228 (2024)

[47] Radu, F.A., Pop, I.S., Attinger, S.: Analysis of an Euler implicit-mixed finite element scheme for reactive solute transport in porous media. Numerical Methods for Partial Differential Equations: An International Journal **26**(2), 320–344 (2010)

[48] Brooks, A.N., Hughes, T.J.R.: Streamline upwind/Petrov-Galerkin formulations for convection dominated flows with particular emphasis on the incompressible Navier-Stokes equations. Computer methods in applied mechanics and engineering **32**(1-3), 199–259 (1982)

[49] Burman, E.: Consistent SUPG-method for transient transport problems: Stability and convergence. Computer Methods in Applied Mechanics and Engineering **199**(17-20), 1114–1123 (2010)

[50] John, V., Novo, J.: Error analysis of the SUPG finite element discretization of evolutionary convection-diffusion-reaction equations. SIAM journal on numerical analysis **49**(3), 1149–1176 (2011)

[51] Hairer, E., Hochbruck, M., Iserles, A., Lubich, C.: Geometric numerical integration. Oberwolfach Reports **3**(1), 805–882 (2006)

[52] Sanz-Serna, J.M.: Symplectic integrators for hamiltonian problems: an overview. Acta numerica **1**, 243–286 (1992)

[53] Wilson, A.B., Wang, J., Jenkins, E.W., Husson, S.M.: Numerical simulation of solid phase adsorption models using time-integrated, up-winded finite element strategies. Computing in Science & Engineering **22**(3), 64–78 (2018)

[54] Adams, R.A., Fournier, J.J.: Sobolev spaces (2003)

[55] Ervin, V.J., Kubacki, M., Layton, W.J., Moraiti, M., Si, Z., Trenchea, C.: On limiting behavior of contaminant transport models in coupled surface and groundwater flows. Axioms **4**(4), 518–529 (2015)

[56] Layton, W.: A connection between subgrid scale eddy viscosity and mixed methods. Applied Mathematics and Computation **133**(1), 147–157 (2002)

[57] Fix, G.J., Gunzburger, M.D., Peterson, J.S.: On finite element approximations of problems having inhomogeneous essential boundary conditions. Computers & Mathematics with Applications **9**(5), 687–700 (1983)

[58] Brenner, S.C., Scott, L.R.: The mathematical theory of finite element methods **3** (2008)

[59] Chrispell, J.C., Ervin, V.J., Jenkins, E.W.: A fractional step θ-method for convection–diffusion problems. Journal of Mathematical Analysis and Applications **333**(1), 204–218 (2007)

[60] Arbogast, T., Wheeler, M.F.: A characteristics-mixed finite element method for advection-dominated transport problems. SIAM Journal on Numerical Analysis **32**(2), 404–424 (1995)

[61] Radu, F.A., Pop, I.S.: Mixed finite element discretization and Newton iteration for a reactive contaminant transport model with nonequilibrium sorption: convergence analysis and error estimates. Computational Geosciences **15**(3), 431–450 (2011)

[62] Barrett, J.W., Knabner, P.: Finite element approximation of the transport of reactive solutes in porous media. part ii: Error estimates for equilibrium adsorption processes. SIAM Journal on Numerical Analysis **34**(2), 455–479 (1997)

[63] Dawson, C.: Analysis of an upwind-mixed finite element method for nonlinear contaminant transport equations. SIAM Journal on Numerical Analysis **35**(5), 1709–1724 (1998)

[64] Protter, M.H., Weinberger, H.F.: Maximum principles in differential equations (2012)

[65] Burkardt, J., Trenchea, C.: Refactorization of the midpoint rule. Applied Mathematics Letters **107**, 106438 (2020)

[66] Nochetto, R.H., Verdi, C.: Approximation of degenerate parabolic problems using numerical integration. SIAM Journal on Numerical Analysis **25**(4), 784–814 (1988)

[67] Arbogast, M.F. T.and Wheeler: A nonlinear mixed finite element method for a degenerate parabolic equation arising in flow in porous media. SIAM Journal on Numerical Analysis **33**(4), 1669–1687 (1996)

[68] Woodward, C.S., Dawson, C.N.: Analysis of expanded mixed finite element methods for a nonlinear parabolic equation modeling flow into variably saturated porous media. SIAM Journal on Numerical Analysis **37**(3), 701–724 (2000)

[69] Siddiqua, F.: Spurious numerical dissipation and time accuracy. PhD thesis,

University of Pittsburgh (2024)

[70] Grisvard, P.: Elliptic problems in nonsmooth domains (2011)

[71] Gunzburger, M.D., Hou, S.L.: Treating inhomogeneous essential boundary conditions in finite element methods and the calculation of boundary stresses. SIAM Journal on Numerical Analysis **29**(2), 390–424 (1992)

[72] Dupont, T., Scott, R.: Polynomial approximation of functions in Sobolev spaces. Mathematics of Computation **34**(150), 441–463 (1980)

[73] Dauge, M.: Elliptic boundary value problems on corner domains: smoothness and asymptotics of solutions **1341** (2006)

[74] Scott, L.R., Zhang, S.: Finite element interpolation of nonsmooth functions satisfying boundary conditions. Mathematics of Computation **54**(190), 483–493 (1990)

[75] Brezis, H.: Functional analysis, Sobolev spaces and partial differential equations, 599 (2011)

[76] Evans, L.C.: Partial differential equations (graduate studies in mathematics, vol. 19) **67** (2009)

[77] Schwartz, J.T.: Nonlinear functional analysis, 236 (1969). Notes by H. Fattorini, R. Nirenberg and H. Porta, with an additional chapter by Hermann Karcher

[78] Gilbarg, D., Trudinger, N.S.: Elliptic partial differential equations of second order, 517 (2001). Reprint of the 1998 edition

[79] Thomée, V., Wahlbin, L.: On the existence of maximum principles in parabolic finite element equations. Mathematics of Computation **77**(261), 11–19 (2008)

[80] Dale A., J.C.T., P., R.H.: Computational fluid mechanics and heat transfer (2012)

[81] Layton, W., McLaughlin, M.: Doubly-adaptive artificial compression methods for incompressible flow. Journal of Numerical Mathematics **28**(3), 175–192 (2020)